To the Graduate Council:

I am submitting herewith a dissertation written by Nancy Gail Kincaid entitled "Ultrastructural and Functional Effects of Lead Poisoning on Adult Canine Myocardium: Assessment of Thiamin Treatment." I have examined the final copy of this dissertation for form and content and recommend that it be accepted in partial fulfillment of the requirements for the degree of Doctor of Philosophy, with a major in Animal Science.

Robert G. Schaub, Major Professor

We have read this dissertation
and recommend its acceptance:

Accepted for the Council:

Vice Provost
and Dean of the Graduate School

ULTRASTRUCTURAL AND FUNCTIONAL EFFECTS OF LEAD POISONING ON ADULT CANINE MYOCARDIUM: ASSESSMENT OF THIAMIN TREATMENT

A Dissertation

Presented for the

Doctor of Philosophy

Degree

The University of Tennessee, Knoxville

Nancy Gail Kincaid

August 1985

DEDICATION

To my whole family, I dedicate this work. To Steve, my husband and friend, words can not express my gratitude for your love, encouragement and belief in me. To Cheryl, my daughter, you gave me another important reason to finish this work. I am grateful to my parents for instilling in me the love of learning as well as for their constant love and to my sister for always being there to listen and encourage.

ACKNOWLEDGMENTS

In the course of dissertation research, a number of people have assisted me generously. I am indebted to Professors Gerald R. Bratton, R.L. Murphree, John R. Kennedy and Hugo Eiler, my committee and in particular to Robert G. Schaub who served as my chairman and friend. I would like to express sincere appreciation for their guidance and encouragement throughout the course of this study.

I hereby acknowledge with thanks the permission granted by Academic Press and the editors, G.W. Richter and M.A. Expstein to quote copyrighted material (1973) page 11, from Pathological Effects of Lead by R.A. Goyer and B.C. Rhyne, in International Review of Experimental Pathology 12:1-77, 1973.

ABSTRACT

The effects of lead (Pb) poisoning on the adult canine myocardium were assessed quantitatively using stereological techniques, functional testing, and blood analyses as well as qualitatively by morphological investigation. Subacute (chronic, but lethal) lead poisoning was studied in fifteen adult dogs divided into three groups: control, Pb treated (Pb given in ascending amounts from 50 mg/kg to 200 mg/kg Pb per day for up to 9 weeks) and Pb + vitamin B_1 treated (Pb given as described above and thiamin given at a dose of 100 mg/kg i.m. daily). Relative measurements using stereological techniques compared the volume fractions of cellular components of the three groups. Blood was analyzed for lead, hemoglobin, hematocrit, total erythrocytes, total leukocytes, thiamin pyrophosphate (TPP), delta-aminolevulinic acid dehydratase activity (ALAD), and zinc protoporphyrin (ZPP).

The major finding of the stereological analysis was the statistically significant increase of 3.2% in myofilament volume in the Pb treated group and the significant decrease in mitochondrial volume in both the Pb treated and Pb + B_1 treated groups. A statistically significant decrease in the mitochondria/myofilament volume ratio was found in the Pb treated, but not Pb + B_1 treated group. This may indicate either a protective effect of thiamin on mitochondria or a reduced compensatory need of the myocyte to increase myofilament volume.

Control values for mitochondrial and myofilament volumes were consistent with published reports on canine left ventricular myocardium.

Electron microscopic observations alone showed no morphological differences in mitochondria or other cellular components between treatment groups. A trend toward decreased function was noted only in the Pb treated group by a decrease in the first derivative of ventricular pressure (dp/dt at 50 mmHg developed isovolumic pressure) and by a decrease in peak ventricular pressure. Thiamin had little effect on the animals' clinical status. Tissue and blood lead levels did not indicate a protective effect of thiamin. TPP levels were found to significantly increase in Pb treated animals and rise even higher in Pb + B_1 treated animals. In dogs from both lead treated groups, ALAD activity decreased to less than 10% of initial values and ZPP levels increased slightly.

TABLE OF CONTENTS

LIST OF TABLES

LIST OF FIGURES

CHAPTER I

INTRODUCTION

Man's present knowledge of the effect of lead exposure or poisoning on the cardiovascular system is inadequate. Perhaps of even greater importance is the need to further investigate the effect of lead on individual cells in an attempt to determine how lead produces systemic toxicity. The lead concentration in cardiac tissue following lead poisoning is low compared to that of bone, kidney, liver and spleen. However Barltrop et al. (7) state that

> The toxic effects of the metal are not always directly related to its affinity for a particular tissue; thus, the terminal encephalopathy of lead poisoning is in contrast to its low affinity for cerebral tissue.

Very few ultrastructural studies have focused on the heart, yet this tissue can be used as a sensitive indicator of the ultrastructural activity of lead. The heart might serve as an example of how lead affects other cells. Since damage produced by lead is usually not the primary cause of death, myocardium would be easier to study. This is especially important when thiamin (Vitamin B_1) or other compounds are tested for their possible prophylactic or therapeutic potential. In addition, myocardial tissue heals poorly, lacks the ability to regenerate new myocardial cells, and is replaced by fibrous tissue when acutely damaged.

Cardiovascular disease is prevalent in our society, and the utilization of lead is rapidly increasing. Kopp et al. (76) suggest

> Because environmental stressors that contribute to the deterioration of the heart would pose significant health problems, evidence demonstrating compromised cardiac function and metabolism induced by chronic heavy metal exposures would suggest that lifetime cadmium and/or lead exposure may contribute to the development of degenerative cardiovascular disease states.

It is important to investigate this possibility because of the threat of expanding pollution.

The purpose of this study is to investigate the effect of lead on canine myocardial ultrastructure and to quantitate these changes using stereological techniques. The second objective is to observe how thiamin would effect these changes.

CHAPTER II

LITERATURE REVIEW

1. LEAD POISONING

There has been a decline in cases of severe lead intoxication, however, the high level of general pollution poses a principal threat to human health today (49). Lead, unlike most metals, has no essential function in the body, only toxic effects.

Lead Exposure

Lead toxicity may occur in man through occupational exposures where there is use or manufacture of ammunition, bearings, brass, bronze, pipes, storage batteries, solder cables, lead shielding, pigments, chemicals or processed metals (120). Worker exposure in these industries occurs mainly through airborne exposure (26). Other sources of lead poisoning as reviewed by Cullen et al. (26) include ingestion of moonshine whiskey, lead paints, battery burning, bullet retention, ceramic making, eating from unfired pottery, cooking in leaden pots, home abortifacients, target shooting, lead-containing herbal medicines and cosmetics, and soldering.

Lead poisoning in animals according to Bartik and Piskac (6) of of the University of Veterinary Medicine in Czechoslovakia, is most frequently encountered in ruminants, followed by horses, poultry, dogs, cats and pigs. In Tennessee and Texas, dogs and cattle account for 99% of the cases of lead poisoning, followed next by horses, with lead

poisoned cats and pigs very rarely seen (10). This lead is ingested as used motor oil, lead powder or scrap, and lead deposited on vegetation as a result of motor vehicles.

The typical current levels of inorganic lead found in the ambient environment from industrial waste and gasoline exhaust are not felt to be causes of major health risks for adults, although there are concerns over the effects of these low levels in children (26). This is because children (23) and young rats (79) absorb more lead from the gastrointestinal tract, up to 50% and perhaps higher, while human adults absorb only 5 to 10% of ingested lead (106). The proportion of inhaled lead that is absorbed in the body is more difficult to determine, but studies of lead deposition report values of 36 and 46% (71) depending on particle size and other factors.

Lead, once it is absorbed, is only slowly metabolized, stored and excreted. The resident time of lead in blood and soft tissue is about 35 to 40 days (106,107); while the resident time of lead incorporated into bone is 25 to 30 years (23). A number of dietary factors influence the absorption of lead (23,25,49). Excessive amounts of protein and fat and deficiencies of protein, calcium, phosphorus, iron, zinc, and vitamin E are factors known to enhance lead toxicity (84). Milk diets in calves increase the absorption and retention of lead over hay and grain diets (135). Since up to 10% of ingested lead is absorbed in man (106), approximately 90% is eliminated in the feces. In man, absorbed lead is primarily excreted in the urine (54-78%), however, hair, nails, sweat, and salivary, gastric, pancreatic and biliary secretions with feces total approximately 25% (107). In

contrast, sheep excrete more lead in bile than in the urine (10). Urinary excretion of lead is increased by sodium citrate, ascorbic acid, calcium ethylenediaminetetraacetic acid (Ca-EDTA) (25) and thiamin (86).

Lead Concentrations

Ong (96) has reported that approximately 94% of lead in human blood is bound to erythrocytes, mostly attached to the hemoglobin molecule of the beta-chain. Only 6% is in plasma and most of that is in the albumin fractions (83). Blood lead levels are primarily used in the diagnosis of lead poisoning, but Chisolm (22) feels they are more reflective of the intensity of the most recent lead exposure than of the body lead burden. Goyer and Rhyne (56) stated in 1973 that

> Blood lead concentration is probably the single most useful measure of lead toxicity since increased blood lead concentrations reflect soft tissue concentrations which relate to adverse functional or metabolic effects.

The Center for Disease Control in 1978 gave four classes of blood lead levels to be used for determining the risk for children (18), but not for clinical diagnosis:

Normal - less than 30 µg (microgram) Pb/100 ml whole blood

Moderate Risk - 30 to 49 µg Pb/100 ml whole blood

High Risk - 50 to 69 µg Pb/100 ml whole blood

Urgent Risk - 70 µg and above Pb/100 ml whole blood

Piomelli et al. in 1984 considered children with blood lead levels greater than 70 µg/100 ml, symptomatic or asymptomatic, to be

experiencing lead intoxication and recommended prompt treatment with BAL and Ca-EDTA (104). Children with blood levels of 56 to 69 µg/100 ml should also be treated, but treatment limited to Ca-EDTA only. Blood lead levels of 25 to 55 µg/100 ml in children should require the Ca-EDTA provocation test to assess the lead excretion ratio. Only blood lead levels of less than 25 µg/100 ml were considered normal.

Three phases of lead toxicity have been described for adults by Goyer and Rhyne (56). These are used as diagnostic criteria and are based on blood lead concentrations:

"Normal"/no clinical effects - < 40 µg Pb/100 ml whole blood

Subclinical or adaptive - 40 to 80 µg Pb/100 ml whole blood

Clinical toxicity - > 80 µg Pb/100 ml whole blood

Chisolm (20) states that virtually all cases of severe acute lead poisoning, including those with acute encephalopathy, are associated with blood lead concentrations of 100 µg Pb/100 g whole blood or greater. Blood lead must be correlated with other biochemical, functional or clinical manifestations of lead toxicity.

The concentration of lead in various organs in normal and lead intoxicated persons is shown in Table I. The largest deposit of lead is usually found in bone, bound in a nondiffusible form (56). The bones store up to 95% of all lead retained in the body of chronically poisoned adult humans. The diffusible fraction of lead from plasma enters and leaves capillaries, permeates cell membranes, and enters cells of the central nervous system, liver, kidneys and other organs. Only trace amounts of lead are normally present in muscle and brain

TABLE I

LEAD CONTENT OF TISSUE FROM 15 PERSONS WITH NO ABNORMAL EXPOSURE TO LEAD (CONTROLS) AND PERSONS DYING FROM LEAD INTOXICATION[a,b]

Tissue	Controls	Lead Intoxication
Bone	0.67–3.59	5.6–17.6
Liver	0.04–0.28	1.8–8.0
Kidney	0.02–0.16	0.6–5.5
Spleen	0.01–0.07	1.13
Heart	0.04	0.2–0.8
Brain	0.01–0.09	0.24–1.2

[a] As reviewed by Goyer and Rhyne (109) and adapted from that article. Permission granted by Academic Press to use copyrighted (1973) material.

[b] Values are the ranges in milligrams per 100 gm of wet tissue.

tissue, and even in lead poisoning, these levels change very little in comparison to the levels found in kidney and liver. This may occur because of the excretory function of the kidneys and liver (56).

Clinical Symptoms of Lead Poisoning

Acute lead poisoning in man results most often in intestinal disorders characterized by anorexia, indigestion, constipation, colic and diffuse pain in the abdomen (25). Acute lead encephalopathies are rare in adults (25) and have recently become rare in children (104). Vomiting, apathy, drowsiness, stupor, ataxia, and convulsions characterize acute encephalopathy. Severe cases result in coma with cessation of breathing and heart action (25). Acute encephalopathy carries a significant mortality and results in severe permanent brain damage in a least 25% of survivors (20). Lead in blood in acute encephalopathy can range upward from 80 µg/100 ml (21).

The clinical symptoms of acute poisoning in dogs include vomiting, anorexia, tender abdomen, diarrhea, constipation, hysteria, convulsions, ataxia, blindness and mydriasis (6). Cattle and horses poisoned by lead show anorexia, severe nervous depression, possible paralysis of the limbs, sometimes blindness, abdominal pain and convulsions (6). In addition, symptoms in horses described by Bratton (10) include laryngeal hemiplegia (roaring), hyper-excitability, and ataxia. Young calves acutely poisoned over 20 days or less showed depression followed by periods of hyperexcitability, anorexia, pharyngeal paresis, hypoglossal paresis, muscle tremors,

generalized muscle weakness, hyperesthesia, ataxia, blindness, and teeth grinding (13).

Chronic lead poisoning in man is more common than the acute form and the onset of symptoms is slower. Signs include muscular weakness, marked feelings of total exhaustion, drowsiness, aversion to food, sleeplessness, weariness in the lower extremities, constipation (25) and sometimes pain in the joints and limb muscles (26,83).

Piomelli et al. (104) in 1984 stated that "The vast majority of children with lead poisoning now referred to pediatricians from screening clinics are asymptomatic."

The Nervous System

Subclinical lead intoxication is becoming more important as knowledge about the effect lead has on the developing nervous system becomes greater. Chisolm (23) maintains that

> There is a worldwide consensus that blood lead concentrations maintained during the preschool years in excess of 50 µg. Pb/100 ml. whole blood carry an unacceptable risk for subtle but long-lasting impairment of the nervous system.

Gerber (49) has reviewed the studies that suggest that mental retardation is more frequent and intelligence scores are lower in children from lead-intoxicated mothers and that children at relatively low exposure levels may have a lower intelligence, abnormal fine motor control, hyperactivity, and hyperexcitability. It is known from studies of acute encephalopathy that the nervous system is particularly sensitive to lead. The most prominent pathological changes noted in the brain are cerebral edema associated with an increase in

cerebrospinal fluid pressure, proliferation and swelling of endothelial cells accompanied by dilatation of capillaries and arterioles, proliferation of glial cells and focal necrosis and neuronal degeneration (56).

Peripheral nervous system lesions include a decreased conduction velocity in motor and sensory nerves (25). Motor paralysis of the extensor muscles causing the typical syndrome of wrist and ankle drop, (49) as well as some degree of muscle weakness can occur (56). Lampert and Schochet (81) studied segmental demyelination and remyelination in rats poisoned by lead and felt that lead-induced peripheral neuropathies were related to Schwann cell degeneration and proliferation.

The Hematopoietic System

The abnormalities of hematopoiesis induced by lead poisoning are confined to the red cell series and anemia, a late sign of industrial lead poisoning, can be slight to moderately severe (1). Three main enzymes of heme synthesis are affected by lead. The cytoplasmic enzyme delta-aminolevulinic acid dehydratase (ALAD) which catalyses the condensation of two molecules of aminolevulinic acid (ALA), decreases with increasing blood levels (36). ALAD is a sensitive indicator of recent lead exposure and can show alterations even when no clinical signs are noted (49). It can be used in conjunction with blood lead values.

Ferrochelatase, the enzyme which inserts an iron atom into protophyrin IX to make heme is the second enzyme effected by lead

(36). Less sensitive to lead than ALAD, its inhibition can lead to the formation of zinc protoporphyrin (ZPP) in place of the heme. Even low amounts of ZPP can be detected with great sensitivity, making blood ZPP levels very useful as a screening test for chronic lead poisoning. ZPP fluoresces and with the use of a specialized hematofluorometer, the amount of ZPP-globin in whole blood can be quickly determined. In addition, the ZPP incorporated into the reticulocyte in the course of hematopoiesis is retained by erythrocytes for their lifespan (36).

The third enzyme inhibited by lead is coproporphyrinogen decarboxylase and like ferrochelatase, it is a mitochondrial enzyme that is lost before the erythrocytes are released from the bone marrow (47).

Gastrointestinal and Hepatic Systems

While colic, constipation and diarrhea have long been associated with lead poisoning, the mechanism of action is not yet clear (26,49). Gerber et al. (49) reviewed the studies that showed that the defense mechanisms of the body are affected by lead. They concluded that the susceptibility to bacterial and viral infection is enhanced and the resistance to injected endotoxin is reduced, probably as a result of a toxic action of lead on the liver.

Renal System

The pathological effects of lead on the kidneys of man and animals has been reviewed by Goyer and Rhyne (56). Acute intoxication results in cloudy swelling and some cellular necrosis, the proximal convoluted tubular cells are the most severely affected. It is controversial

whether lead relates to the chronic form of renal disease which occurs in man. Kehoe (72) stresses that little evidence has been found in American industry of any undue incidence of chronic nephritis among workmen in the lead industries. The situation is similar for lead intoxication in childhood resulting in chronic lead nephropathy in adulthood (56,72). Most investigators have failed to find an increase in frequency of hypertension and chronic renal disease in men occupationally exposed to lead (as reviewed by Goyer and Rhyne, 56). There appears to be a relationship between gout and lead nephropathy and a study Goyer and Rhyne reviewed suggested that lead-induced gout might be mediated by excessive tubular reabsorption of urate (56).

Characteristic intranuclear inclusion bodies are formed in the proximal tubular epithelial cells of the kidneys in lead intoxication (24,53). The nuclear inclusion bodies can be found as early as 24 hours after a single intraperitoneal injection of lead (24). They consist of a dense central core and an outer fibrillary zone; they vary in size and the fibrils do not have periodicity (53). Their formation appears to be a universal response to an excessive body burden of lead. While they are commonly found in kidneys, they have been observed in liver, osteoclasts, and astrocytes in animals given large doses of lead (53).

The inclusions consist of a lead-protein complex, the protein a non-histone acidic protein (53). The lead content of mitochondria is low compared to the nuclear content. It could be functionally important to keep the cytoplasmic lead concentration low, especially the lead concentration of mitochondria. This could be accomplished by

binding lead in a non-diffusible or nontoxic form within the intranuclear inclusion body and allowing the cells to stay viable (52). Lead inclusion bodies are removed by chelation with EDTA (57,90).

Endocrine and Reproductive Manifestations

It has been recognized for over a century that women working in lead industries are more prone to sterility, abortions and unhealthy offspring (26,49). Cullen et al. (26) reviewed studies that showed an increase in both premature deliveries and in premature membrane rupture in a lead mining region. These authors reviewed studies which showed a significant dose relationship between lead exposure and decreasing sperm counts, decreasing sperm motility and increasing proportion of abnormal sperm in men with different levels of lead exposure. During fetal development, the placenta is only a partial barrier to lead and lead is found distributed among organs in the fetus the same as in the adult, the highest concentrations in bone and liver and smaller but significant concentrations in blood, placenta, brain, kidney and heart (as reviewed by 49). The effects of lead on development seem to be caused by the toxic action on the embryo (49). Gilfillan (51) has proposed that one of the main reasons for the decline of the Roman Empire was that the upper class and wealthy leaders developed living habits which resulted in lead poisoning. Lead intoxication resulted in a very rapid decline in the birth rate and the number of surviving children of the Roman upper class.

Experimental results on the mutagenic action of lead are often contradictory and do not allow a satisfactory evaluation of the genetic risk. The results do not seem to furnish unequivocal proof for the mutagenic action of lead (49).

2. CURRENT TREATMENTS OF LEAD POISONING

EDTA, BAL, d-penicillamine

The first recommendation for the treatment of the lead poisoned patient, human or animal, is removal from further lead exposure. For acute manifestations such as encephalopathy or colic, the intramuscular use of the Ca chelate of ethylenediaminetetraacetic acid (EDTA) and 2,3,-dimercaptol-1-propanol (BAL) in combination or intravenous calcium EDTA alone is according to Chisholm (20) the recommended treatment for humans. This is immediately followed by oral d-penicillamine which according to Chisolm (20) "virtually always obviates the need for repeated courses of parenteral chelation therapy." This treatment is also used for asymptomatic individuals with blood levels greater than 100 µg Pb/dl. For chronic manifestations in humans, d-penicillamine or intermittent calcium EDTA is advocated. EDTA is the currently recommended drug of choice for treatment of lead poisoning in animals (6).

The adverse treatment effects with calcium EDTA include hypokalemia, proteinuria, microscopic hematuria and large epithelial cells in the urinary sediment, hypercalcemia, and fever (20). Nausea and vomiting are the main toxic effect of BAL. Side effects reported with d-penicillamine include transient eosinophilia, erythematous skin

rashes, superficial extravasations of blood, fever, prolonged bleeding time, leukopenia, agranulocytosis, thrombocytopenia, and nephrotic syndrome (20). D-penicillamine may also enhance absorption of lead still present in the gastrointestinal tract and interfer with vitamin B_6 metabolism (as reviewed by 14). Chisholm (20) states that these potential risks can be minimized by assuring adequate hydration and urine output and by careful monitoring of blood and urine during adminstration of the drugs.

DMSA, DMPS

Recently meso-dimercaptosuccinic acid (DMSA) and 2,3-dimercapto-1-propanesulfonic acid, Na salt (DMPS) have been recommended as possible antidotes for heavy metal poisoning, including lead poisoning (3). DMSA and DMPS have been studied extensively in the People's Republic of China, the Soviet Union, and Japan. These compounds are water soluble chemical analogs of BAL, but in contrast to BAL, they have less toxicity, greater water solubility, limited lipid solubility, and are effective when given orally. In a study comparing DMSA, d-penicillamine and EDTA for their influence on tissue lead concentrations in mice pretreated with Pb acetate, DMSA was the most effective at decreasing tissue lead (43). The absorption of lead from the gastrointestinal tract was not influenced by DMSA (59). Five lead-poisoned smelter workers treated with DMSA had blood lead levels that dropped from 97 to 43 µg/dl with no side effects or renal toxicity detected (44). Based on the results by Bratton et al. (14), Aposhian

(3) suggested the prophylactic potiental of DMSA and DMPS be studied alone and in combination with thiamin to prevent lead poisoning.

Thiamin

The use of thiamin (Vitamin B_1) for prophylaxis and treatment of lead poisoning in animals has only recently been studied. Bratton et. al (13) found that calves dosed with lead acetate and given 100 mg/day of thiamin showed no clinical signs of lead poisoning while four of five calves on the same dose of lead without thiamin showed clinical signs and two died. Tissue levels of lead in kidney, liver, cerebral cortex, and sciatic nerve were significantly lower, 2 to 10 times less in the lead-thiamin group than in the lead-only group. A significant reduction in lead concentration of the heart, spleen, vastus lateralis muscle, and bone was not shown. The blood lead levels in the lead-only group were considered diagnostic of lead poisoning while the levels in the thiamin-lead group remained within the normal range. Delta-amino-levulinic acid dehydratase activity decreased by 70% during the study and was not affected by thiamin. Thiamin in some way prevented the deposition of lead, especially in the kidney, liver and brain. Bratton et al. (13) postulated that the mechanism by which thiamin interferes with lead deposition in tissue could be interference with lead absorption, due to complex formation of lead with thiamin or one of its metabolites followed by subsequent excretion, or by enhanced transportation of lead from soft tissue to bone. A followup study by Bratton and Zmudzki (12) used lead poisoned calves that were subsequently treated with thiamin and/or Ca-EDTA. Results showed the

lead concentration in blood and tissues decreased in direct proportion to the Ca-EDTA levels only and while thiamin seemed to increase the rate of recovery and improve the physical signs, a significant synergistic effect of thiamin with Ca-EDTA could not be shown.

Sasser et al. (109) studied the effect of thiamin on lead absorption in the rat and found that thiamin facilitated absorption and increased the amount of lead initially taken up by the tissue. They found that thiamin also promoted more rapid release of lead from tissues. The absence of elevated lead levels in the urine of thiamin-treated rats suggested that the excess lead was not excreted in the urine.

Louis-Ferdinand et al. (86) reported that concomintant lead (10 mg/kg i.p.) and thiamin (T), (20 mg/kg s.c.) administration to adult mice did not alter the 24 hour fecal excretion of lead, but did increase by 70% the urinary output of lead. In weanling rats receiving lead and thiamin concomitantly, blood, brain, bone, kidney and liver lead levels were 26 to 37% lower than in rats receiving lead alone. According to Louis-Ferdinand et al. (86):

> Results suggest: (1) acute Pb lethality is not affected by concomitant T administration; (2) T treatment of lead-burdened animals increases blood Pb initially, perhaps by alteration of soft tissue distribution; (3) the tissue Pb lowering effect of T administered concomitantly is not the result of decreased Pb absorption.

An ultrastructural study by Mollenhauer et al. (90) compared kidney tissue from lead-dosed-untreated, lead-dosed-thiamin treated and lead-dosed-Ca-EDTA treated calves (pretreated with lead for seven

days). Lead deposits were found in nuclei and mitochondria of proximal tubular cells of untreated and thiamin treated calves, but not in EDTA treated calves. EDTA treatment was accompanied by a generalized disorganization of cellular ultrastructure and mitochondria damage, a change not seen in thiamin treated animals. While some calves died in the untreated group, the EDTA and thiamin group of calves remained in good general health.

The use of thiamin by Bratton et al. (13,14,) in the treatment of lead poisoning was empirical. It is known that thiamin plays three major roles at the cellular level. A primary function is to act as a cofactor for three enzymes involved in carbohydrate metabolism (pyruvate dehydrogenase, alpha-ketoglutarate dehydrogenase and transketolase) (93). An important function of thiamin pyrophosphate (TPP) is in oxidative decarboxylation of alpha-keto acids, pyruvate, and alpha-ketoglutarate. The second role for thiamin is concerned with biosynthesic pathways as reflected by the transketolase reaction of the pentose phosphate shunt yielding nicotinamide adenine dinucleotide phosphate (NADPH) and pentose (93). The third role involves the metabolism and function of excitable membranes and nerve conduction (93).

The precise interaction of lead and thiamin in the body is unknown. Tokarski and Reio (118) reported that prolonged administration of lead acetate decreases the thiamin level in lead treated rats and diminishes the enzymatic activity of pyruvate dehydrogenase as well as that of erythrocyte transketolase. Blood pyruvate levels increase by

about 20% and oxidative decarboxylation of pyruvate by liver mitochondria decreases.

To determine the thiamin statis of a person or animal, the erythrocyte transketolase activity can be measured. A direct measurement of TPP, the functional form of thiamin, is a more sensitive indicator of thiamin status (121).

Moran and Green (93) state that "True toxicity to thiamine has not been described in man." Doses of 500 mg (intravenous) have been tolerated in man (93) and doses up to 400 mg/kg have been tolerated in dogs in a preliminary trial (unpublished results).

3. ULTRASTRUCTURE OF CARDIAC MUSCLE

To determine the effects of lead on heart tissue, knowledge of normal cardiac ultrastructure is essential. Cardiac muscle is striated, but unlike skeletal muscle, it consists of a functional syncytium of small individual cells (115). Individual cells branch and are mainly attached end-to-end at specialized regions called intercalated discs (Figure 1). While all muscle cells are capable of contraction and conduction of electrochemical impulses, most are specialized for contraction. Contractile cells contain a high concentration of filamentous protein and moderate amounts of glycogen and in mammals have a diameter of 10 to 15 μm (micron). The conductive cells, Purkinje cells, have fewer filaments, a higher concentration of glycogen and larger diameters. Cells have also been described which are intermediate in morphological characteristics and probably

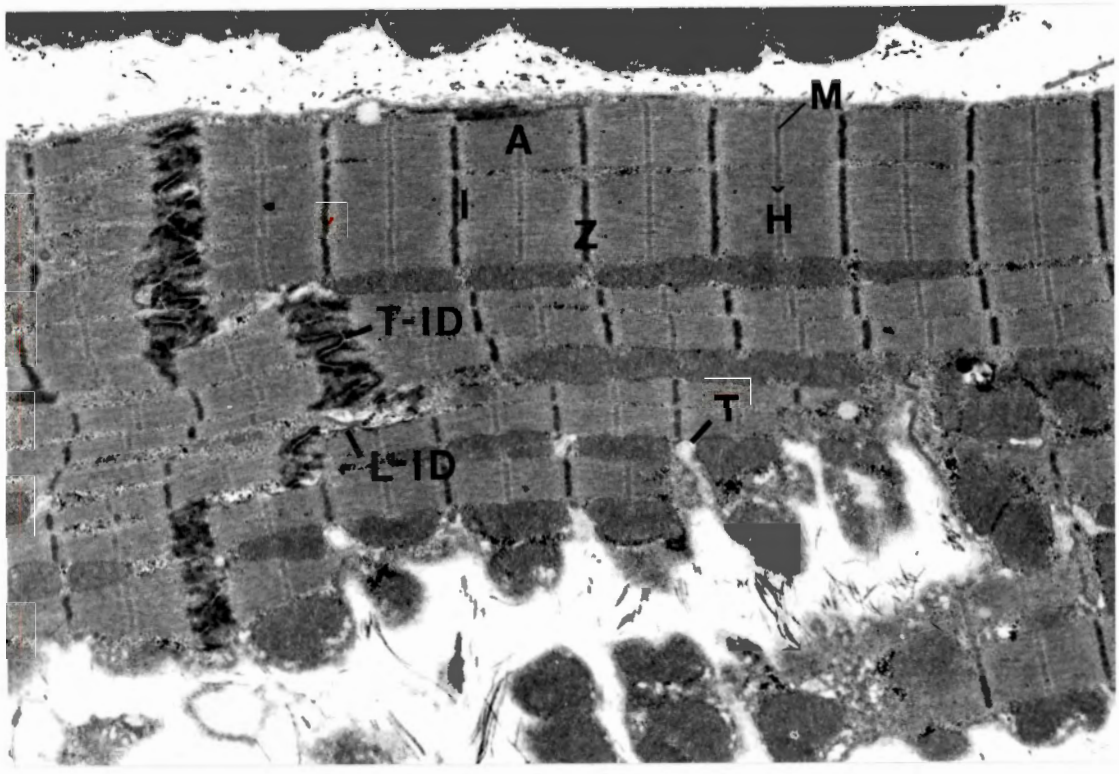

FIGURE 1. Myocardial sarcomeres. Each sarcomere is bounded by two z lines (Z) and contains an A band (A), I band (I), H zone (H) and M band (M). Longitudinal (L-ID) and transverse (T-ID) portions of an intercalated disc are seen. An invagination of the sarcolemna, the T tubule (T) is also evident. (X9,600)

represent the finest ramifications at the terminus of the conductive system of the heart (87).

Nonmuscle cells are important for cardiac function. These include fibroblasts and cells of capillaries and lymphatics. Sympathetic nerves ramify in both the atrial and ventricular myocardium and parasympathetic nerves are found in atrial myocardium and regions of the ventricular conduction system (82).

Contractile Cells

Contractile cells usually contain one fusiform, centralized nucleus orientated along the long axis of the cell (Figure 2). Canine myocardium often has binucleate cells (82). The nuclei contain predominantly euchromatic chromatin and prominent, active, nucleoli. The nuclear envelope consists of two membranes interrupted by nuclear pores approximately 800 A (angstrom) in diameter which are covered by thin diaphragms. A thin layer of heterochromatin lines the nucleoplasmic surface of the nucleus. The nuclear envelope is often infolded into the nucleoplasm (82). All myocytes are present shortly after birth when division ceases. Remaining growth, approximately a 17 fold increase in weight for humans, occurs by hypertrophy.

The Golgi complex can be found near the nucleus. The smooth vesicles of the Golgi are approximately 500 to 800 A in diameter, are limited by a single membrane, usually are not electron dense and probably serve a transport function (82). Coated vesicles or bristle-coated vesicles probably serve as transporters specialized for protein. Multivesicular bodies found in myocardial cells probably have

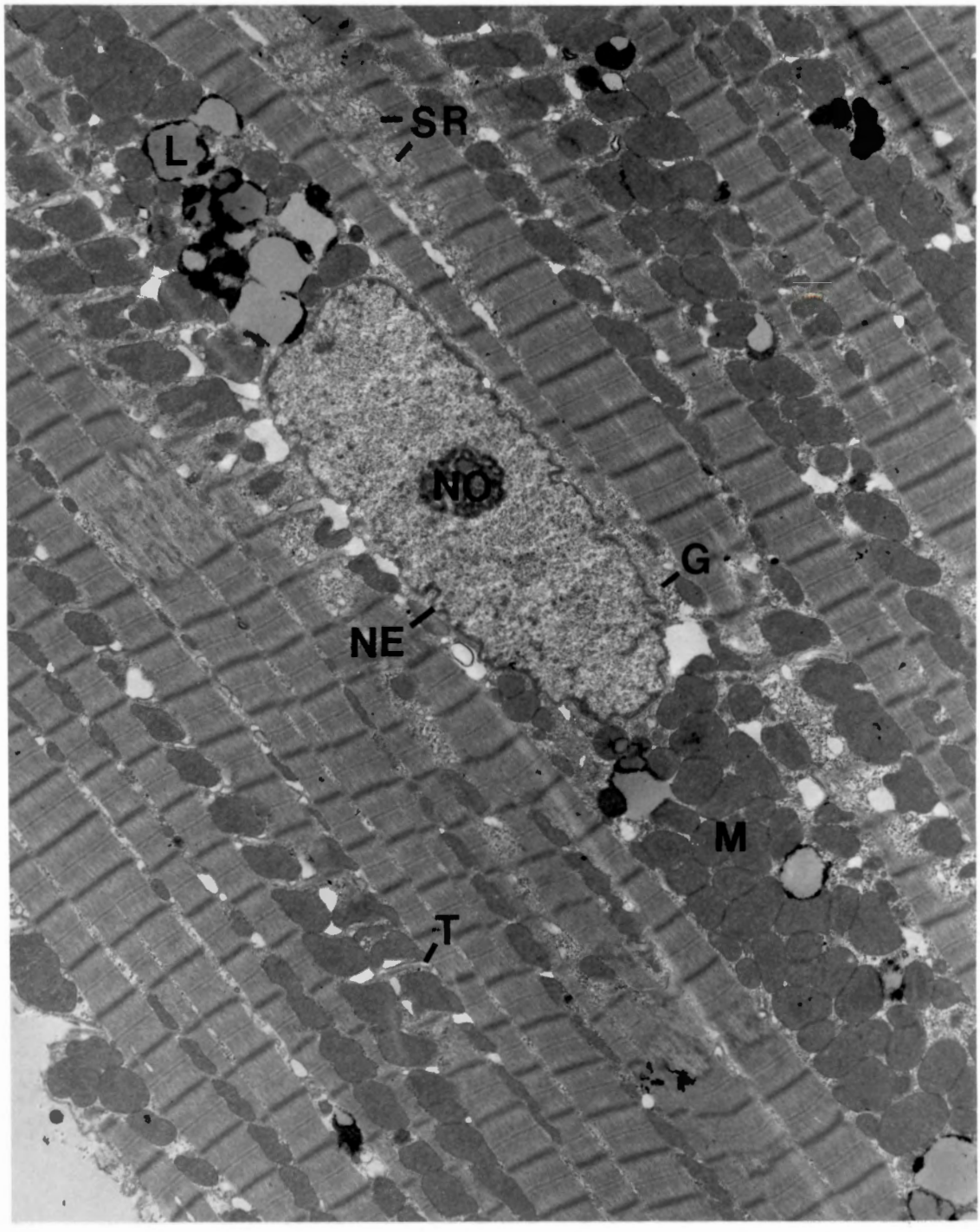

FIGURE 2. Cardiac papillary muscle from a control dog. Nuclear envelope (NE), nucleolus (NO), mitochondria (M), lipofuscin (L), glycogen (G), sarcoplasmic reticulum (SR), T tubule (T). (X7,000).

lysosomal activity. Small vesicles approximately 500 A in diameter are found within the large vesicles of approximately 0.1 μm in diameter.

Lipofuscin bodies are membrane bound vesicles containing heterogeneous deposits of electron dense material usually located near the conical cap of the nucleus (Figure 2)(82). They contain the insoluable breakdown product of lipids and phospholipids, the complexes left after lysosomal enzymes of autophagic vacuoles have finished their presumed role in the turnover and renewal of cellular organelles. Lipofuscin bodies are probably the result of autophagic digestion of the membranes of aged mitochondria, endoplasmic reticulum, and possibly other organelles. The amount of lipofuscin increases with age or with atrophic diseases of the heart (82).

Cardiac muscle is striated, meaning the contractile material is divided into repeating units about 2.2 μm long called sarcomeres (Figure 1). Each sarcomere is bounded by two Z lines and contains substriations which are generated by the myofilaments, comprising interdigitating thick filaments (myosin) and thin filaments (actin) arranged in such a way as to form bands, the A bands and I bands respectively (Figure 1). The A band contains thick myosin filaments, 150 A in diameter and 1.5 um long and an H zone consisting of only myosin filaments. In the M band, the myosin is cross-linked by the M protein to six other myosin filaments.

The I band is composed of thin, f-actin filaments, 50 to 80 A in diameter and 1 μm long as well as troponin and tropomyosin, proteins important for regulating the interaction between thick and thin filaments (82). About half of the actin overlaps the A band. The

actin filaments seem to be fastened to the Z lines at one end. The free ends slide between the myosin filaments during the contraction-relaxation cycle.

Table II lists some of the parameters of ventricular myocardial cells described by the percent they occupy of the cell volume. The myofilaments occupy between 48 and 52% of the cell volume in many studies on rat ventricular myocardium, however, a study by Friedman et al. (45) reported a volume of 64%. One study in calves reported a myofilament volume of 39% (102 as cited by 29). Studies on canine left ventricular tissue show a 54 to 57% volume for myofilaments (50,88). Human biopsy tissue from patients with non-ventricular-loading diseases such as mitral stenosis, atrial septal defect and foramen ovale persistens was reported to have a myofilament volume of 47% for youths (age 5 to 15) and 52% for adults (age 42 to 78)(41).

Mitochondria, largely respondible for the aerobic production of chemical energy in the myocardium, are found evenly distributed and closely applied to the surface of the myofilaments (Figure 2, p 21) (82). The mitochondria have an outer limiting membrane and an inner membrane folded into many cristae. The mitochondrial matrix is electron dense and contains small granules, 300 to 400 A in diameter, thought to be sites of calcium storage (99). The appearance of the cristae and matrix are dependent upon the physiological state and conditions of fixation, especially oxygen tension. Mitochondria are pleomorphic and can enlarge or contract, branch and produce small processes or fuse with each other (70). They are frequently 2 to 8 μm long and several micrometers wide in their main portion (82).

TABLE II

PARAMETERS OF VENTRICULAR MYOCARDIAL CELLS
IN VOLUME PERCENT

Species	Myofibrils	Mitochondria	T System	SR*	Cytsol	+ Nucleus
Rat[a]	**	27				
Rat[b]	48	34	1.2	3.5	13	
Rat[c]	48	36	1.0	3.5	12	
Rat[d]	64	36				
Rat[e]	52	38				
Rat[f]	54	33	0.9	4.9	7	
Mouse[g]	**	48				
Guinea pig[h]		24				
Dog[i]	57	25	1.2	2	13	1.5
Dog[j]	54	26	0.87			
Dog[k]	**	25				
Calf[l]	39	31				
Human***,[m]	52	35				2.2

* Sarcoplasmic Reticulum

** Data not available.

*** Human biopsy tissue from patients with non-ventricular-loading diseases such as mitral stenosis, atrial septal defect and foramen ovale persistens.

[a] From Bozner A, Meessen H: Die freinstruktur des herzmuskels der ratte nach einmaligem und nach wiederholtem schwimmtraining. Virchows Arch Abt B Zellpath 3:248-269, 1969.

[b] From Page E, McCallister LP, Power B: Stereological measurements of cardiac ultrastructures implicated in excitation-contraction coupling. Proc Nat Acad Sci USA 68:1465-1466, 1971.

[c] From Page E, McCallister LP: Quantitative electron microscopic description of heart muscle cells. Am J Cardiol 31:172-181, 1973.

TABLE II (CONTINUED)

[d] From Friedman I, Moravec J, Reichart E, Hatt PJ: Subacute myocardial hypoxia in the rat. An electron microscopic study of the left ventricular myocardium. J Mol Cell Cardiol 5:125-132, 1973.

[e] From Datta BU, Silver MD: Cardiomegaly in chronic anemia in rats. Lab Invest 32:503-514, 1975.

[f] From Anversa P, Loud AV, Giacomelli F, Wiener J: Absolute morphometric study of myocardial hypertrophy in experimental hypertension. II Ultrastructure of myocytes and interstitium. Lab Invest 38:597-609, 1978. 38:597-609, 1978.

[g] From Herbener GH, Swigart RH, Lang CA: Morphometric comparison of the mitochondrial populations of normal and hypertrophic hearts. Lab Invest 28:96-103, 1973.

[h] From Plattner H, Tiefenbrunner F, Pfaller W: Cytomorphometric and biochemical differences between the muscle cells in atria and ventricles of the guinea pig heart. Anat Rec 167:11-16, 1970.

[i] From Gerdes AM, Kasten FH: Morphometric study of endomyocardium and epimyocardium of the left ventricle in adult dogs. Am J Anat 159:389-394, 1980.

[j] From McCallister LP, Daiello DC, Tyers GFO: Morphometric observations on the effects of normothermic ischemic arrest on dog myocardial ultrastructure. J Mol Cell Cardiol 10:67-80, 1978.

[k] From Papadimitriou JM, Hopkins BE, Taylor RR: Regression of left ventricular dilation and hypertrophy after removal of volume overload. Morphological and ultrastructural study. Circ Res 35:127-135, 1974.

[l] From Pape C, Kubler W, v.Smekal P: Morphometrie am reizleilungssystem und arbeitsmyocard des kalbsherzens. Beitr pathol Anat u allg Pathol 140:23-37, 1969.

[m] Fleischer M, Warmuth H: Ultrastructural morphometric analysis on normal loaded and on hypertrophied human myocardial left ventricles, in Bolte H-D (ed): Myocardial Biopsy. Berlin, Springer-Verlag, 1980, pp 49-52.

Mitochondria occupy different volumes of the myocardial cell depending on the rate of energy utilization. Rapidly beating hearts generally have a greater mitochondrial volume, while slower beating hearts of larger mammals have less mitochondrial volume (70,82). Table II lists the mitochondrial volume in rats as 34 to 38%, guinea pigs as 24%, calves as 31% and dogs as 25 to 26%. One study of human biopsy samples from patients with non-ventricular-loading diseases found mitochondrial volumes of 35% (41).

Normal myocardial cells contain spherical lipid droplets, approximately 0.1 μm in diameter. They are frequently found closely applied to the outer mitochondrial membrane and often near the region of the I band, probably the result of the preferential location of mitochondria adjacent to the A band (82). The lipid droplets are dynamic stores of triglycerides and are used during acute exogenous substrate deprivation. Their levels increase as a result of an increased level of free fatty acids in the blood during adrenergic stimulation (82).

Glycogen, small, dense granules (beta-particles) 150 to 350 A in diameter are found in higher concentration in cardiac muscle than in skeletal muscle (Figure 2, p 21)(82). Glycogen is found in the conical caps of cytoplasm near the nucleus, in the interstices of the myofilament lattice in the I band, in the clefts of sarcoplasm in the myofilament mass (82) and in subsarcolemmal sites (64).

Ribosomes, 150 to 200 A electron-dense granules are found predominantly free in the cytoplasm (82). The ribosomes are more

apparent when the glycogen has been hydrolysed during preparation of the tissue for observation.

Myocardial cells are covered by the sarcolemma, a 75 to 90 A unit membrane. The glycoprotein coat, 500 to 800 A in diameter, is anchored to the plasma membrane and may influence the local ionic environment at this membrane by concentrating and holding ions such as calcium (82). The sarcolemma frequently shows prominent indentations (64).

Myocardial cells are aggregated into bundles by a variety of lateral intercellular connections. These include in addition to large collagen struts and intercalated discs, an elaborate network of connections including the following components: cell coats, collagen fibrils, 8 to 10 nm (nanometer) diameter microfibrils, 10 to 40 nm diameter granules and 3 to 6 nm diameter microthreads (108).

Mammalian working fibers have transverse tubules (T tubules) which are the invaginations of the sarcolemma along the Z lines (Figure 2, p 21)(115). The T tubule of cardiac muscle, in contrast to that of skeletal muscle, is lined by a glycoprotein coat and is much larger, 1000 A as apposed to 400 A in diameter respectively (60). The T tubules are absent in conductive fibers, atrial fibers and immature mammalian fibers (115). Cardiac muscle has one T tubule per sarcomere at the Z line while skeletal muscle has two per sarcomere, one at each A-I junction. In addition to transversely orientated tubules, longitudinal connections exist between successive T tubules along the length of the cell (82).

The sarcoplasmic reticulum (SR) is a lacelike intracellular network of tubules measuring 20 to 60 nm in diameter (Figure 2, p 21)

(115). It is devoid of attached ribosomes and closely applied to the surface of the myofilaments (82). The SR contains an ATP-dependent pump that moves calcium from the cytoplasm into the lumen of the SR network against a gradient (115).

Cardiac muscle SR differs from skeletal muscle SR in three ways (115):

1. the cardiac muscle SR is widely continuous from one sarcomere to the next;
2. close apposition between specialized regions of the SR (the junctional SR of the couplings), in cardiac muscle occurs both at the T tubule and at the surface sarcolemma;
3. the fine structure of these appositions in cardiac muscle is different from that of presumable homologous structures in skeletal muscle in some respects. Cardiac junctional SR is not dilated and is not a large site for calcium storage.

The intercalated disc is the specialized end-to-end attachment of two sarcolemmas across a thin interspace. Dense transverse portions of the disc are attached to less conspicuous longitudinal segments. Each disc is made up of fascia adherens (intermediate junctions), macula adherens (desmosomes) and nexus ("gap" junctions). At the fascia adherens, the largest portion of the transverse segments, the two plasma membranes are parallel and separated by a 200 to 300 A interspace containing proteinaceous material. The actin filaments of the I band enter the filamentous mat that lies adjacent to this junctional membrane (82). The macula adherens are round-to-discoid shaped attachments of the plasma membranes. The plasma membranes are

separated by a 250 to 300 A interspace filled with a dense proteinaceous material, frequently exhibiting a central dense stratum. Cytoplasmic filaments (tonofilaments) 100 A in diameter are attached to the desmosome.

Nexus can be located on the transverse portions of the intercalated disc, but they are usually located on the longitudinal segment, parallel to the myofilaments. The nexus consists of two plasma membranes composed of globular subunits arranged in a hexagonal array and separated by a 20 A gap. The nexus electrically couple cells by permitting low resistance passage of ions from cell to cell which allows the wave of membrane depolarization to pass from cell to cell and provide for the coordination of the contraction of individual cells (82).

Atrial contractile cells are smaller in diameter than ventricular cells and often lack a well-developed T tubule system, a species dependent characteristic. Mammalian atrial cells contain a highly developed Golgi complex, a relatively high proportion of rough endoplasmic reticulum and numerous membrane-bound storage granules approximately 0.1 μm in diameter, called specific atrial granules (30). It has recently been shown that diuretic and natriuretic activity of rat atrial extracts is largely stored in secretory-like granules found in atrial cardiocytes, presumably the specific granules (30,31). Injection of extracts from atrial muscle caused a rapid, more than 30-fold increase of sodium and chloride excretion, and a 10-fold volume increase of urine and a doubling of potassium excretion in rats (30). The atrial extract has also been shown to cause

relaxation of isolated vascular and nonvascular smooth muscle preparations (27). It is possible that the atria can detect volume changes and release substances that influences renal function and vascular tone (27). A control mechanism has been suggested by de Bold and Flynn (31) in which the heart would participate in the maintenance of water and electrolyte balance and thus play an endocrine role. It must be proved that the atria can detect an increase in the extracellular fluid volume and respond by releasing bioactive substances into the bloodstream that stimulate a rapid loss of fluid through the urine and peripheral vasodilation (27).

Specific granules have also been described to a lesser extent in the ventricular cells of some species (82,115). Schipp and Wehren (115) describe dense granules in amphibians which seem to contain catecholamines.

Purkinje Cells

An action potiental arises within cells of the sinoatrial node, passes through atrial myocytes to the atrioventricular node and is conducted through the collagenous septum to the ventricles by Purkinje cells. Nodal cells are smaller in diameter than ventricular cells, lack T tubules, have fewer peripherally located myofilaments, have larger amounts of glycogen and smaller mitochondria (82). Purkinje cells are larger in diameter, but otherwise resemble nodal cells (82). Pape et al. (102 as cited by 29) compared the volume percent of myofilaments in calves and found a volume of 39% in left ventricular working fibers and 21% in left crus Purkinje fibers. The volume

percent of mitochondria followed the same pattern for ventriclar working fibers and Purkinje fibers, 31% and 11% respectively. Additional quantitative ultrastructural data can be found in a book by H. David (29).

4. MYOCARDIAL CELL INJURY

With certain infections and toxic etiologies, the mechanism leading to cardiac failure is probably simple cell destruction. The myocardium heals poorly and the adult heart lacks the ability to regenerate new myocardial cells. Severe cellular damage leads to necrosis and eventually to replacement of contractile tissue by fibrous tissue (70). However, simple cell death accounts for a minority of cardiomyopathies. Abnormalities of any of the contractile proteins or any of a number of calcium transport processes could give rise to the reduced contractility that characterizes the cardiomyopathies. Defects in any of the reactions involved in energy production also adversely affect the myocardium (70).

Sustained hemodynamic overloading of the heart is the most common cause of depressed myocardial function (70). The overloading can be caused by systemic or pulmonary hypertension, valvular heart disease, or loss of functional myocardial tissue from ischemic heart disease (70).

Hypertrophy

Hypertrophy is a major response of the heart to chronically increased hemodynamic demands. Hypertrophy results in expansion of

muscle tissue not from new cells but rather from an increase in the size of each existing myocyte (2,70). The percentage of cell volume made up of myofibrils was increased approximately from 47% to 54% in studies of cellular hypertrophy resulting from experimentally produced hypertension in rats (98,100). In the same studies the percent of cell volume occupied by mitochondria decreased from 36% to 33% (98,100). The increase in myofibrillar volume results in an increased need for energy consumption. This is occurring at the same time a decrease in mitochondrial volume is taking place, which results in less energy in the form of ATP being produced. This disproportion, carried out over time may be important in the ultimate development of heart failure by the hypertrophied myocardium (98). The mitochondrial to myofibril ratio is frequently used as an index for characterizing hypertrophic changes (2). While increasing in the early stages of hypertrophy, the ratio generally decreases with prolonged hypertrophy. This ratio of mitochondrial volume to myofibril volume was decreased significantly from 0.627 to 0.534 in endocardial samples of hypertrophy in rats, but not significantly (0.602 to 0.563, $p < 0.1$) in epicardial samples of the same study (2).

An increase in cell volume causes another problem, in that the ratio of external sarcolemmal membrane per unit of cell volume falls, from 36% to 32% in rats (98). Vital functions performed by the external sarcolemma such as nutrient uptake, waste product elimination and movement of ions associated with electrical excitation might be affected. The membranes of the T tubule system attempt to compensate for this by increasing in order to keep the ratio constant between

sarcolemma-T system membrane and cell volume (2,98). The percent of cell volume occupied by sarcoplasmic reticulum remains approximately constant in the enlarged cells, however, the surface area of the sarcoplasmic reticular membrane increases significantly. As a result, the sarcoplasmic reticular membrane area and myofibrillar volume increase proportionately so that their ratio remains constant. Anversa et al. (2) found an absolute increase in sarcoplasmic reticular volume and surface, nearly double the increase in myofibrillar mass, possibly compensating for the reduced calcium binding capacity of this system in hypertrophy. The sarcoplasmic reticulum grows proportionately more than the cell as a whole (98). Anversa et al. (2) summarized the cellular reaction in hypertrophy as one in which myofibrillar, sacoplasmic reliculum and T tubule system growth exceeds the mean cellular growth while nuclear, mitochondrial and matrix growth is relatively less.

In addition, endocardial and epicardial myocytes respond with different magnitudes of cellular and subcellular hypertrophy; epicardial myocytes respond more while endocardial myocytes exhibit greater vulnerability to ischemic episodes (2). Hypertrophy is a result of an increased demand for mechanical work among an increased number of contractile elements. There is a decrease in energy expenditures of each unit and this provides for effective cardiac pumping, up to a certain point. The newly formed contractile units within the enlarged cells are not completely normal, and the strength of each unit is decreased, for reasons not fully understood (70).

Ischemic Heart Disease

Ischemic heart disease, most commonly arising from arteriosclerosis with a narrowing of the coronary arteries, results in a decline in myocardial contractility. The heart has virtually no oxygen stores so the loss of the substrate oxygen is felt within one minute and results in a loss of contractility to the anoxic area (70). Glycogen stores remain intact, but the store of fats increase after an interruption of the blood supply. The ratio of glycolysis increases, however it is only transient and probably due to an accumulation of NADH and a lack of NAD (70). Periods of 40 to 60 minutes of ischemia produce cell death apparently due to a decrease in ATP needed to maintain key ion pumps (70,75). Cell death is likely caused by damage to the sarcolemma, the membrane being unable to maintain normally low intracellular levels of Ca^{++}. These changes in calcium fluxes between intracellular and extracellular spaces may account in part for the loss of contractility in the ischemic heart (70).

Tissue water and electrolytes are unaffected by 40 minutes of ischemia, but when reflow is allowed, H_2O, Na^+, Cl^- and Ca^{++} increase and K^+ and Mg^{++} decrease intracellularly (126). Intramitochondrial Ca^{++} increases and there is a release of CPK and other lysosomal enzymes into the blood stream probably as a result of membrane disruption (46).

Morphological changes develop with ischemia of 40 minutes or more. Anoxia without reflow of blood causes moderately swollen myocardial cells (75), clumping and margination of nuclear chromatin (66,75), and relaxation of myofibrils (75). Many mitochondria appear swollen with

abnormally clear matrices, while others have reduced cristae with irregular fragments. Irregular, dense amorphous matrix densities measuring up to 80 nm in diameter appear in many mitochondria (64,75) and probably represent a reorganization or denaturation of mitochondrial structural material rather than an accumulation of exogenous material (75). The sarcolemmal membranes and intercalated discs remain intact. Lysosomes and T tubules usually appear unaltered (64).

Mitochondrial volume changes are reported in studies of cardiopulmonary bypass resulting in ischemic arrest. A study by Partin et al. (103) shows an increase from 25% to 40% in the mitochondrial volume with 20 minutes of ischemia. At 30 minutes the mitochondrial volume drops to 31%. In contrast, McCallister et al. (88) reported a decrease from 26% to 19% in mitochondrial volume from hearts after one hour of normothermic ischemic arrest. The myofibrillar volume fraction also significantly decreased from 54% to 37% in ischemic hearts and the T system volume fraction decreased from 0.87% to 0.51% (88). These volume changes are probably the result of myocardial cell swelling secondary to intracellular edema.

The membrane surface area of the sarcoplasmic reticulum (SR) relative to the volume of the SR was evaluated by McCallister et al. (88) and found to be significantly increased, indicating the SR may fragment into smaller vesicles. The surface area to volume ratio for the T system also increased, indicating the T system had vesiculated. This is probably the result of lysosomal action.

When restoring the circulation to an area temporarily occluded for 40 minutes or more, the morphological picture changes. Contraction bands, the result of contraction of several sarcomeres with a thickening of the Z bands (66,75) can be observed. The usual parallel organization of myofilaments is lacking in some places (75). Cell swelling is evident with subsarcolemmal blebs lifting the sarcolemma away from the myofibrils (66). Vacuoles are formed (75), the larger ones often containing remnants of mitochondria. Mitochondrial swelling is evident with occasional fragmentation (66,75). Giant mitochondria apparently formed by fusion are found in subsarcolemmal and intermyofibrillar locations (110). Also granular densities, in addition to the amorphous, flocullent densities previously described are observed in mitochondria, granules presumably composed of calcium (66,75). The granular densities measure up to 300 nm, often have an annular appearance and often appear to be partially or totally surrounded by cristae. Both amorphous densities and granular densities can be observed in the same mitochondrion or the same cell (75). With advanced stages of anoxia, mitochondria show marked swelling of the inner compartments. More rarely mitochondria show abnormal condensation of the inner compartment with relative enlargement of the intermembrane space. Schiaffino et al. (110) also describes paracrystalline inclusions in the intermembrane space of mitochondria due to anoxic changes. Lysomes and intercalated discs appear normal after a brief reflow period, however the sarcolemma covering blebs is often incomplete (64,75).

Cardiotoxic Chemicals

Cardiotoxic chemicals can cause cell injury and induce lesions in two different ways. Catecholamine analogs which are adrenergic beta-receptor agonists can cause focal myocardial necroses due to hemodynamic changes brought about by their pharmacological effects (5). In contrast, certain drugs like the anthracycline antineoplastic drugs have a true autonomous cardiotoxic effect which is independent of the cardiovascular pharmacological action. Allergic reactions involving several organs in addition to the heart have also been described. In addition, functional alterations can be caused by chemicals that induce molecular changes without producing morphological lesions (5). Lesions are produced by changes in hemodynamics brought about indirectly by the vasodilating antihypertensive agents hydralazine, diazoxide, minoxidil and others as well as directly by the adrenergic beta-receptor agonists isoproterenol, salbutamol (5), epinephrine and norepinephrine (40). Both types of drugs result in adrenergic stimulation which causes an augmented transmembrane calcium influx and subsequent increase in the rate and force of contraction. With energy and oxygen requirements increasing, the drugs also cause hypotension which may result in hypoxia in the least perfused area of the heart, the subendocardial zone of the left ventricle including the papillary muscles.

The lesion resulting from a single dose of isoproterenol is first seen in rats within minutes and consists of irregular contraction bands with rupture of the myofibrils (5). Swelling of the mitochondria is followed by the appearance of electron dense granules, probably

calcium. Other organelles become displaced and disintegration of the sarcolemma and of entire myocytes occur. Areas of hyaline necrosis and of myocytolysis with macrophages and fibroblasts are found 8 to 24 hours after a single dose of isoproterenol. The lesions produced by multiple dosing are not more extensive than those caused by one or two doses and the lesions heal and may not recur during continuous dosing.

In a study (40) using overdoses of isoproterenol, epinephrine, and norepinephrine in rats, glycogen is reduced, but returns to normal in non-necrotic fibers. The lipid pattern is similar with an increase in lipid droplets initially, with a eventual decrease to normal levels in non-necrotic cells. Swelling of the sarcoplasmic reticulum is evident. The myofibrils show a thickening of the Z lines, with progressive loss of density resulting in indistinct myofilaments and striations. Mitochondrial swelling and loss of cristae are found. Lysosomes increase throughout the myocardium, but are especially prominent in cells adjoining the necrotic areas. Cells resembling plasma cells and macrophages are evident usually closely associated with the capillaries. Similar lesions are produced by minoxidil, a vasodilating antihypertensive agent.

Electrocardiographic examination is helpful in the assessment of cardiac effects resulting from isoproterenol. These include marked sinus tachycardia, arrhythmias, and ST segment depression in dogs. The presence of necrosis is correlated with ventricular extrasystoles occurring 24 hours after treatment (5).

Direct cardiotoxicity of chemicals is the second way lesions are produced in the myocardium (5). Daunorubicin and doxorubicin, two

highly effective antineoplastic agents of the anthracycline type are drugs whose therapeutic usefulness is limited by their cardiotoxicity. Acute cardiotoxic effects consist of hypotension, tachycardia and various arrhythmias and chronic toxicity is seen as severe congestive heart failure. In acute toxicity, nucleolar segregation is seen in the myocytes, suggesting damage to the DNA leading to interference with synthetic processes. In chronic cardiotoxicity, the morphological damage is widespread. There is lysis of the myofilaments and swelling of the sarcoplasmic reticulum producing vacuolization of the cytoplasm. There is accumulation of lipid and dilation of the T tubular system. The intercellular junctions separate, leaving hemidesmosomes, intracytoplasmic junctions and spherical microparticles exposed. Mitochondria are not uniform, some decrease in size, and changes in matrix density can be observed. Concentric lamellae or myelin figures composed of electron-dense material are found in some mitochondria. While cellular atrophy is present, the inflammatory reaction usually is absent or minimal. Calcium-containing intramitochondrial inclusions have not been demonstrated unequivocally in toxicity resulting from daunorubicin or doxorubicin adminstration.

Lead Intoxication

Lead has been shown to affect the cardiovascular system, however the exact site of action or the extent of its involvement in cardiovascular disease is still unknown. Whether lead directly injures myocardial cells or indirectly affects them by affecting the blood supply to the heart is not known. Stofen (116) reviewed the research,

predominantly European, on the effect of environmental lead on the heart. Research directed toward the influence of lead on the cardiovascular system began in the 18th century. In the 19th century, Planches (116) stressed lead as a vascular poison. Tscherkess et al. (as cited by 116) claimed lead induced vascular narrowing, the extent of which correlated with the lead concentration. Zapel (as cited by 116) and Froboese (as cited by 116) found severe degenerative changes of the aorta and of coronary, renal and cerebral arteries in workers with lead poisoning. Cantarow and Trumper (as cited by 116) published a comprehensive survey of literature on the vascular effects of lead. In addition to arteritis and hemorrhage at various sites, the possibility of necrosis was mentioned. According to the majority of reports cited, vascular damage included arteriosclerosis, degenerative and fatty changes of the intima and media and proliferation of the perivascular connective tissue, especially in renal vessels. Minden (as cited by 116) observed myocarditis and intimal hypertrophy in the hearts of rabbits chronically poisoned with lead.

Karstad (69) described myocardial lesions in naturally and experimentally lead-poisoned waterfowl. The lesions observed were infarct-like, usually without leukocyte infiltration. Necrotic muscle fibers lost definition and stainability and were replaced by fibrous connective tissue. Interstitial fibrosis, small scattered scars in both the endocardium and epicardium were observed. It appeared the apparent damage to the arterioles was acute and the damaged myocardium was replaced by fibrous connective tissue. Carlson and Nielsen (17) found necrosis and degeneration of the skeletal and myocardial muscle

fibers of mallard ducks treated with lead and diets low in calcium and other nutrients.

Interstitial fibrosis with a serous exudate and relatively few inflamatory cells was described by Kline (74) as chronic myocarditis in five human patients with lead poisoning. Cloudy swelling of the myocardial fibers was the most outstanding change in addition to the new formation of connective tissue compressing and replacing adjacent muscle fibers. Kline considered the primary lesion to be vascular although no blood vessel changes were observed. Myocarditis was the terminal cause of death in two of the five patients and probably the contributing cause of death in the others.

Other observations on the damage due to lead poisoning observed at the light microscopic level include those of Kosmider and Srocznski (77 as cited by Freeman, 42). They found a loss of definition of the muscle structure with degenerative changes of the muscle fibers and focal fibrosis, however an inflamatory exudate was seen only in one case. Smigla (114) observed in guinea pig hearts a protein degeneration with infiltration of "little cells" (possibly small lymphocytes) and an increase in the thickness of vessel walls. Hard evidence for a vascular origin of myocardial damage is lacking.

Electron microscopy of lead poisoned myocardium shows changes not apparent with light microscopy. The most consistant and obvious changes are mitochondrial, including swelling, slight with low blood lead levels (91,92) and moderate to severe (two-to-three fold) with higher lead levels (4,73). Many mitochondria lose their relatively regular spacing and orientation (4,73,91) and show abnormal clumping

interspersed by areas of rarefaction of the matrix (91,92). Khan (73) described some mitochondria with disoriented cristae, vacuolation, and a granular to dense intramitochondrial matrix increase. A few mitochondrial cristae showed lumpy or linear condensation and an increased electron density, while others were swollen and had short and marginal cristae. Matrical granules were homogeneous and occasionally tended to clump.

Moore (91,92) using low levels of lead found only minor myofibrillar changes with some loss of structural definition of the myocardium as a whole. High levels of lead produced diffuse degenerative changes including myofibrillar fragmentation with separation by edema fluid (4,73). Myofibrillolysis was especially prominent in areas adjacent to intercalated discs with indistinct Z lines (73). Where myofilaments were intact, Z lines showed focally interrupted, sawtoothed architecture. The intercalated discs showed an increase in convolutions with segmental disruptions and disjunctions and a widening of the intermembranous spaces. An increased number of lipid droplets associated with mitochondria were observed (73).

Moore (91,92) did not see specific changes in lysosomes, nuclei or membrane systems with low levels of lead. With higher lead levels, a dilation of the sarcoplasmic reticulum (73) with a loss of the normal orientation with the sarcomere and the Z lines was observed (4). Nuclear changes were the first morphological alterations noted by Khan (73) at the lowest blood levels. These changes included peripheral and membranous condensation of nuclear chromatin and nucleolar disorganization with loss of distinct nucleolonema. Clusters of

chromatin consisting of granular and fibrillar components were seen possibly as newly aggregated chromatin or disorganized nucleoli. Interchromatin granules also increased in numbers. Nuclear inclusions found in lead poisoned kidney tubule cells are not seen in heart tissue (73). Mitochondrial changes are the most commonly reported and nuclear changes the least reported electron microscopic observations.

Electrocardiographic Changes

Morphological changes can only be observed in human autopsy samples or experimental animal studies. The results of myocardial involvement in lead poisoning can be described by electrocardiographic changes and myocarditis in adults, children and experimental animals. Kosmider and Petelenz (78 as cited by 42) have reported electrocardiographic changes in 66% of 38 adults studied. The most frequent changes are flattening of the T waves and depression of the S-T segment, but other changes include shortened P-R intervals, low voltage QRS complexes, and conduction defects. Atrioventricular conduction defects were noted in two adult patients with chronic lead poisoning by Myerson and Eisenhauer (95). After treatment with sodium calciumedetate (EDTA), the patients' electrocardiographic readings returned to normal.

Electrocardiographic changes have been seen in children suffering from lead intoxication. The electrocardiogram of a 3 year old child showed a flattening of the T waves that disappeared by one month after EDTA treatment (42). Silver and Rodriquez-Torres (112) recorded electrocardiographic studies before and after treatment of children

with lead poisoning. Twenty-one patients had one or more abnormal findings before treatment and only four had the abnormalities after treatment. Kline (74) reported chronic myocarditis as the cause of death in two children and a contributory cause in three children with lead poisoning. Four of the children exhibited tachycardia and bradycardia.

Kopp et al. (76) studied chronic, low level lead exposure in rats and found P-R interval prolongations caused by increased conduction time through the His-Purkinje cell system. Lead poisoned rabbits were shown to develop abnormal electrocardiographic patterns, most commonly T wave changes and abnormal QRS complexes (77).

While electrocardiographic changes have been observed in adult humans and animals exposed to lead, little is known about the cardiac effects of chronic exposure early in life. Lead can produce autonomic dysfunction; it can heighten myocardial vulnerability to catecholamine induced arrhythmias. Norepinephrine has been given to test the responsiveness of the adult rat cardiovascular system that was exposed to a critical level of lead during the first 21 days after birth, a time coinciding with the development of adrenergic innervation (62). An intervenous infusion of norepinephrine (80 ug/kg min^{-1}) produced more than four times as many ventricular extrasystoles in lead exposed rats as in controls (62). These studies by Hejtmancik and Williams (61,62) indicated that the direct cardiac effects and the indirect reflex vagal effects of norepinephrine are both involved in the arrhythmogenic responses of lead-exposed animals. Williams et al. (128) reviewed these and other cardiac effects of lead and discussed

possible mechanisms involved including interference with central delta-aminobutyric acid systems, alteration of adrenergic nerve development, and Pb-Ca interaction.

Biochemical Changes

The toxic effects of lead are not always directly related to its affinity for a particular tissue (7). This is likely the case for the physiological effects of lead seen in the heart. Barltrop et al. (7) and Stowe et al. (117) showed that while heart tissue retains relatively little lead as compared to bone, kidney, the reticulo-endothelial system, and the central nervous system, tissue levels are about three fold (117) higher than those found in control dogs. Asokan (4) was unable to show measurable myocardial lead levels in rats when blood lead levels of 110 ug per cent were found along with ultra-structural changes. In general, most studies show higher levels of lead in the liver, kidney and spleen when compared to the heart. Singh et al. (113), however reported higher heart and kidney lead levels compared to liver and brain levels in baby rats who were born of lead poisoned mothers and fed only their mothers milk for three weeks. In a study by Bratton et al. (13), young calves fed a milk replacer diet and treated with lead were found to have a higher level of lead in heart tissue when compared to controls. As reported by others, the concentration of lead in heart tissue was much lower than that found in liver, kidney, or bone.

A considerable portion of lead found in the heart is bound to the mitochondrial fraction (7,111); mitochondria consequently are one of

the potiental sites for the toxic effects of lead. Lead inhibits cardiac mitochondrial oxidative phosphorylation and mitochondrial respiration (16). Goyer and Krall (54) demonstrated decreased respiration and partial uncoupling of oxidative phosphorylation in the mitochondria of kidney tubule cells of lead intoxicated rats. The mitochondria showed impaired respiratory enzyme activity and increased lability because of membrane alterations and impaired energy metabolism. Diaphorase (DPNH), an enzyme associated with electron transfer and aerobic phosphorylation is diminished more in heart than in skeletal muscle following acute lead poisoning (67).

5. STEREOLOGY

Ultrastructural changes which occur in the heart due to toxic substances or ischemia are often graded and in order to adequately evaluate these changes, a quantitative mathematical analysis must be used (88). Stereology has recently been used as a powerful quantitative tool to study the changes which occur in the heart under various conditions (88).

The methods of stereology are used to derive three-dimensional information from an analysis of two-dimensional images using geometrico-statistical reasoning (39,122,129). Stereology, a branch of applied mathematics is an extrapolation from two-dimensional to three-dimensional space using rules and formulas that are mathematically precise (39). Morphometry, a separate area of mathematics, is the measurement of structures (39). Morphometric data

can be obtained using various procedures, but it can also be derived from stereological analysis of tissue sections (122).

Morphometry of a cell, using stereological procedures, provides quantitative information on cellular fine structure, allowing quantitative correlation of biochemical and physiological data with morphological data obtained on structurally intact cells (122). This is important for structure-function correlation.

Stereological methods have only recently been accepted in biology. The earliest stereologists were astronomers (38) while today stereology is used by material scientists, petrographers, physiologists, ceramicists and histologists (39).

Stereological methods have been described to estimate volumes, areas, numbers and sizes of cells or cellular components (129). This is accomplished by superimposing line and point patterns on flat images and counting points and lines which intersect with the component parts under investigation (39). Basic formulas, quite simple and straightforward, are used to analyze the counted points and measured line segments (39). Quantitative relationships exist between the average dimensions of a large number of organelles or particles and those of their profiles on sections (123). In order to describe the relationships, a list of symbols and their definitions is essential. Table III is adapted from a book by Weibel (123) and contains symbols and their dimensions.

Certain fundamental parameters can be used to characterize structures of interest to histologists such as organelles of specific

TABLE III

LIST OF SYMBOLS[a]

Definition	Symbol	Alternative Symbols	Dimensions
1.Parameters of structure			
Volume (of component or structure)	V		cm^3
Surface area (of components)	S		cm^2
Length of linear feature in space	J	L	cm^0
Number of objects	N		cm
Diameter (of spheres)	D		cm
2.Parameters of profiles on section area			
Area of profiles	A		cm^2
Boundary length of profiles (perimeter)	B	L,P,C	cm^0
Transections of linear features	Q		cm^0
Tangents to profile boundary	T		cm^0
Number of profiles	N	n	cm
Diameter (caliper) of profiles	d,h		cm
3.Parameters on test lines			
Length (total) of profiles on test line	L		cm
Intersections with surface or profile boundary	I	P,N,C	cm^0
Length of intercept or chord	l	L_2,L_3	cm^0
Number of intercepts	n	N^2	cm
4.Parameters on test point sets			
Point number on profiles or structure	P		cm^0
5.Parameters of test sets			
Test volume	V_T		cm^3
Test area	A_T		cm^2
Test line length	L_T		cm^0
Test point number	P_T		cm
Section (slice) thickness	t	T	cm
6.Densities in space			
Volume densities	V_V		cm^0
Surface densities	S_V		cm^{-1}
Length density in space	J_V	L_V	cm^{-2}
Numerical density	N_V		cm^{-3}

TABLE III (CONTINUED)

Definition	Symbol	Alternative Symbols	Dimensions
7.Densities on test sets			
Areal density	A_A		cm^0
Boundary length density	B_A		cm^{-1}
Transection density on area	Q_A		cm^{-2}
Numerical density of profiles on area	N_A		cm^{-2}
Tangent density on area	T_A		cm^{-2}
Intercept length density on line	L_L		cm^0
Intersection density on line	I_L		cm^{-1}
Intercept number density	N_L		cm^{-1}
Point density	P_P		cm^0

[a] Table adapted from Weibel ER: Stereological Methods, Vol 1, Practical Methods for Biological Morphometry. New York, Academic Press, 1979.

cell types. Stereology can be used to determine these parameters, parameters which include (124):

V_V: Volume density. Also called the relative or fractional volume, it is the volume of the component of interest related to the volume it is contained in. An example would be mitochondrial volume contained in a unit volume of cytoplasm.

S_V: Surface density. This is the surface area of the component of interest per unit containing volume. An example would be the area of mitochondrial surface per unit containing volume of cytoplasm.

J_V: Line density. This is the length of a filamentous or tubular structure per unit containing volume. An example of this would be the combined length of capillaries in a given organ.

N_V: Numerical density. The number of particles per unit containing volume, an example of which is the number of mitochondria per cell, is referred to as the numerical density.

$\bar{D}$: Mean caliper diameter. The mean distance between parallel planes made to be tangent to the particle over all possible orientations of the particle is referred to as the mean caliper diameter of the structure. An example of this would be the mean diameter of mitochondria or nuclei.

The first three parameters, volume density, surface density, and line density are not dependent on shape, however, numerical density and mean caliper diameter are shape dependent.

The principle of Delesse forms the basis of volumetric determinations which are made by stereology. Delesse, a French geologist, proved in 1847 that the volume density of various components contained in a rock could be estimated on random sections (or slices through the rock) by measuring the relative areas (or areal density A_A) of the profiles (124).

The basic stereological formulas and procedures have been derived by several authors working independently in different disciplines (38). A full history of the basic procedures of stereology is given by Underwood in his book Quantitative Stereology (119).

Basic stereological methods with corresponding formulas exist to estimate the parameters of volume density, surface density, line density, numerical density and mean caliper diameter. To estimate structural parameters one has to decide which test reference system gives the most reliable results. Four choices are available for measuring volume density (124):

1. The relative area occupied by profiles can be estimated directly by planimetry using a polar planimeter or an electronic probe.

2. The cut-and-weigh method requires tracing the profiles onto heavy paper or directly using electron micrographs to cut out and weigh.

3. Linear integration can be used by applying a test line and measuring the intercept lengths, a procedure used in automatic scanning instruments based either on the scan of the specimen stage of the microscope or on a TV scan.

4. A point counting system, simple or semiautomated can be used.

Systematic point counting is often the best method for estimating volume density by stereological methods considering time, cost, and the lower percent coefficient of variation produced (123). The planimetric method of circle fitting and the cut-and-weigh method also gives reliable results on a time-cost basis, but these methods are more useful where the elements of interest are prominent which is usually

not the case with complex structures found in actual micrographs. Often too much work is required on the individual profiles.

The first basic stereological method involves determining volume densities V_V of components under study using stereological formulas found in appendix A-1. The second stereological method involves estimating the surface density S_V. See appendix A-1 for all stereological formulas. When determining surface densities, the objects may have any shape, but they must not be oriented preferentially (structures must be isotropic). The lines of the test system are anistropic and if the structure is also anistropic, error can be introduced. It is possible to use the test system at two orientations (at right angles) to overcome this. Eisenberg (34,35) uses a square lattice test grid oriented at 19^{o} to the fiber axis to overcome systematic errors in the number of intersection counts on orientated membrane systems. The third stereological method is used to estimate linear density J_V. The length per unit volume can be determined for tubules, fibers and filaments by considering them as straight or curved lines in space.

The determinationn of numerical density N_V is more difficult than estimating volume, surface or linear densities. With these three parameters, shape is not important and discrete particles are not necessary (124). This is in contrast to the determination of numerical density and mean caliper diameter $\overline{D}$ where particle shape and size is necessary for the determinations. The estimation of these parameters can be difficult and are truly applicable for spherical particles only (124).

The most difficult stereological problem to solve is determining the size of a particular particle or component or the size distribution of these components (39). In many cases, it is a very important parameter to measure. First the particle shape must be determined and procedures are available (39,122,123,124), however, reasonable satisfactory methods are only available for spherical or near spherical objects. If the shape is spherical, a mean diameter and size distribution can be established using the methods described by Weibel (39,123,124), Williams (129) and Elias and Hyde (39). The determination of size distribution of ellipsoids have been described by De Hoff and Bousquet (32). Their axial ratio should be constant and they should be of the same form (129).

Test Systems

Three fundamental test probes (dp) are needed when applying stereological principles (124):

A_T; test area (dp=2)

L_T: test line (dp=1)

P_T: test point set (dp=0)

To determine which test probe to use for a given task, a probe that forms a trace of dimension dp=0 would be most efficient because the measuring process would be reduced to counting points. When volumetric results are needed, it would seem that measuring areas with planimetry would be more precise. However, statistically this is true only for an individual profile, not a large number of profiles (124).

It is important that many profiles are included in the sample as Weibel explains (123):

> it does not make sense to measure an individual profile with excessive precision if the variation of profile size, or of their areal density on a section, is large from section to section. It is better to work up, in a certain amount of available time, a larger number of fields with rough precision than a small number of fields with high precision, because the number of fields has a greater effect on reducing over-all error than increasing the density of observations on one field.

Point counting is more efficient on a time-cost basis when related to the expected error (124).

The test system that is quite commonly used in point counting consists of a square lattice imprinted on a plastic sheet which is placed over the micrograph. The length of each side of a single square (d) should be chosen such that $d^2 > a_m$ with a_m the area of the largest profile encountered. This insures that no more than one point can fall on the same profile and each point is independent of the other points. This allows the sampling procedure to be statistically described by a binomial distribution (123). The structures in question are not really measured because at the intersection of the grid lines (the point) a sample is considered in or out. While it might appear that this "measurement" would be inaccurate, this is compensated for by the fact that the point set covers a very large sample of profiles, thus securing a representative sample of the whole structure (123). This relies on the fact that the probability of a random point falling on a certain component is given by its volume density, irrespective of the size of the individual profiles.

When rare components are to be studied, it is necessary to use a "d" which is smaller than $d^2 > a_m$ to insure that no profiles remain undetected by the system (123).

A square lattice is commonly employed, however other test systems have been designed to meet specific needs. Weibel (125) describes a multipurpose test system which is composed of discrete short test lines whose end points are arranged in a regular triangular lattice which is an equilateral rhombus. It has its main advantage in surface area estimations. A curvilinear test system designed by Merz (89,108) is composed of semicircles disposed in a square lattice. The advantage this isotropic system has over straight lined systems which have a high degree of anisotropy is that it can be used in estimating the surface of components which themselves show a certain degree of anisotropy, like membranes or boundaries.

The total number of test points to be counted (P_T) is determined by the precision requirements and the approximate volume of the component of interest, a volume roughly estimated on a few micrographs of the appropiate magnification (123). See appendix A-2 for formulas and details.

Random sampling of the tissue is essential and must be considered early in the planning of a stereological study. Weibel (122) has described in detail procedures to assure non-biased results. Stereological measurements, being based on geometrico-statistical principles, are derived from the probability with which section profiles of structures coincide with an appropriate test system. To assure a bias-free random process, rigorous random sampling procedures

must be followed at all stages of a study from choice of animals, through selection of tissue blocks, to recording and analysis of electron micrographs.

Simple random sampling depends on chance for selection of each subsample. Simple random sampling results in a larger standard error when compared to systematic random sampling where dispersion of each subsample is assured by their regular spacing within a sampling lattice. Stratified random sampling, similar to systematic random sampling in the lower standard error produced, also gives good dispersion of samples. With stratified random sampling, equally spaced slices are cut from an organ and each is individually diced. The resulting pool of tissue blocks are processed separately with one or more blocks picked at random from each pool. Each block should provide a single thin section for analysis (122). When micrographs are recorded, they should be fixed to a reference system that is independent of the structures such as a predetermined corner of the mesh of the supporting grid.

The last sampling step involves randomly superimposing a regular lattice on the micrographs. This can be accomplished by placing a transparent sheet with a lattice on it over a printed micrograph or a grid can be photographically placed on a micrograph as it is printed. Alternatively, a negative may be used directly by projecting it on a piece of white cardboard which has the test system drawn on it (122).

Additional measures must be taken to avoid bias in periodic and/or anisotropic samples such as cardiac muscle. Muscle is a highly ordered structure, exhibiting both anisotropy which is the parallel arrangement

of strictly longitudinal myofibrils and periodicity resulting from the alternating arrangements of actin and myosin filaments in the sarcomeres (34). When a longitudinal section is used to sample muscle, periodicity will be revealed and all parts of the periodic structure will be sampled equally (123). The composition of the muscle fiber will be more faithfully represented in a transverse section, however only one region of the element of symmetry will be revealed (123). A compromise exists with an oblique section since it will sample all levels of the periodic structure as well as reveal the composition, however the angle of sectioning can influence the measurements obtained on such a section.

Eisenberg (34) describes a method for evaluating striated muscle. Longitudinal sections are used and a square lattice test grid is oriented at 19^{o} to the fiber axis to overcome systematic errors in the number of intersection counts on orientated membrane systems. However, for strictly volume density measurements, the sectioning angle is unimportant (except that the error introduced by section thickness may be affected by the sectioning angle) (123) and the test lattice can be orientated at any angle (34,97).

CHAPTER III

MATERIALS AND METHODS

Animals

Fifteen male mongrel dogs, 9 months to 3 years of age, 10 to 30 kg in weight were used. The dogs were vaccinated for rabies, distemper, leptospirosis, hepatitis, and parvovirus, and quarantined for two weeks. The Knott's Tests for heartworms were negative and the dogs appeared in good general health. They were housed indoors on concrete runs, fed dry Purina Dog food, and offered water ad libitum.

Treatment

The dogs were randomly divided into three groups of 5 dogs each: Group 1, control; Group 2, Pb treated; Group 3, Pb + B_1 treated. Groups 2 and 3 were treated with lead acetate (Fisher Scientific Co.) mixed in canned dog food and administered in ascending concentrations with time. Each dog was fed 50 mg/kg Pb for 11 days, 100 mg/kg Pb for 17 days, 150 mg/kg Pb for 10 days and 200 mg/kg Pb for 1 to 18 days. The length of treatment and consequently the increasing dosage schedule depended on assessment of the individual animal's intoxicated condition. Animals were killed when neurological signs or severe depression and dehydration were observed. When an animal from one group was killed, one animal randomly chosen from each of the other groups was also killed. Animals in Group 3 received thiamin (thiamin hydrochloride, Butler Co., Columbus, Ohio, NDC No. 11695-7520-0) 100

mg/kg intramuscularly in a divided dose of 50 mg/kg twice daily. The thiamin injections were begun on the same day as the lead treatment. Control animals were fed the same canned dog food without lead, but did not receive any injections of thiamin or the vehicle.

Sampling

Blood was drawn for baseline values before treatment began and again 1/2 hour prior to death for hematological parameters (hemoglobin, total protein, total erythrocytes, total leukocytes) and thiamin pyrophosphate (TPP). In addition to these time periods, blood was drawn weekly for measurement of blood lead concentration, delta-aminolevulinic acid dehydratase activity (ALAD), zinc protoporphrin concentrations (ZPP), and packed cell volume. The dogs were weighed before treatment, weekly, and before death. Each dog was observed daily for general health and clinical signs of lead poisoning.

Analysis

Hematological parameters (hemoglobin, hematocrit, total erythrocyte count, total leukocyte count) were measured by standard methods (Coulter Equipment and Methods Manual, Coulter Electronics, Inc., Hialeah, FL). These parameters were measured by the Clinical Pathology Laboratory, University of Tennessee, Knoxville, Tennessee. Thiamin pyrophosphate was measured to determine thiamin status (121). The assay was performed by Dr. Laken G. Warnock of the Department of Biochemistry, Veterans Administration Hospital, Nashville, Tennessee.

The colometric method of Burch and Siegel (15) was used to determine delta-aminolevulinic acid dehydratase activity in whole

blood, but calculations were performed as described by Chakrabarti et al. (19) and Granick et al. (58). Zinc protoporphyrin was measured directly on a specialized hematofluorometer using front face fluorometry (8).

Blood and tissue samples were analyzed for lead by atomic absorption spectroscopy following dry ashing and organic extraction as described by Yeager et al. (132) and modified by Zmudzki (133). The analysis was performed by Dr. Jan Zmudzki, a Visiting Research Scientist from the Department of Pharmacology and Toxicology, Veterinary Research Institute, Pulawy, Poland.

Physiological function tests

Myocardial function tests were performed prior to treatment and just prior to the animal's death. The dogs were anesthetized with sodium pentobarbitol (30 mg/kg iv) and anticoagulation was achieved by injection of sufficient Na heparin to approximate one unit/ml of whole blood. A standard six lead electrocardiogram (ECG), monitored with electrodes connected to a 9855 Beckman ECG coupler and recorded on a six channel Beckman R-611 Dynograph recorder, was obtained for each animal. The Lead II recording was used for analysis of rate, P-R interval, Q-T interval, and T wave. The left carotid artery was exposed and a high fidelity micromanometer Millar pressure tip catheter connected to a Beckman 9853A pressure coupler and 9979 Dp/dt coupler was inserted into the left ventricle. Left ventricular pressure and Dp/dt (the first derivative of ventricular pressure) were recorded simultaneously. Dp/dt at 50 mm Hg developed isovolumic pressure was

later determined from the recordings. Each dog was assessed for susceptability to development of ectopic electrical activity by the following procedure (62): the right ventricle was cannulated through the right jugular vein and norepinephrine (4μg/kg/min) was infused for 15 minutes. Norepinephrine was discontinued for 10 minutes, the cannula drawn back into the jugular vein, and the norepinephrine procedure repeated. The development of extrasystolic beats was observed and reported as extrasystolic beats/2-minute intervals.

Tissue Sampling

Cardiac tissue was collected for electron microscopy at the conclusion of the heart function tests. While under sodium pentobarbital anesthesia, dogs were placed on a Harvard respirator and the chest opened at the fourth left intercostal space. The heart was quickly removed, rinsed in cold, oxygenated Ringers solution and the left ventral (anterior) papillary muscle excised and placed in 2.5% Tyrode's buffered glutaraldehyde. Longitudinal slices of the papillary muscle were made and trimmed into $1mm^3$ pieces, retaining fiber orientation. Tissue was fixed overnight in glutaraldehyde, then washed in Tyrode's buffer, dehydrated in alcohol, and infiltrated with propylene oxide. The tissue was orientated and flat embedded in a mixture of Araldite and Epon; Appendix C contains additional details.

The remaining heart sample and liver, kidney, bone (femoral head), bone marrow, skeletal muscle, bile, brain stem, cerebral cortex, cerebellum, sciatic nerve, spinal cord, spleen, pancreas, testes, and lung tissue were collected for lead analysis.

Stereological Analysis of Papillary Muscle

Sections one micrometer thick were cut, stained with toluidine blue, and anaylzed to determine tissue orientation. Only transversely or longitudinally orientated tissue was used in the study. Thin sections were cut on an LKB ultratome, stained with uranyl acetate and lead citrate, and examined on a Philips 201 electron microscope. Ten blocks (5 longitudinal and 5 transverse sections) were cut from each animal. Four micrographs from each block were taken at 2,800x and enlarged to 7,000x. Four higher power micrographs of each animal were taken at 29,600x and enlarged to 74,000x. Two high power micrographs focused on paranuclear mitochondria and two on mitochondria located within the myofilament mass; two were transverse and two longitudinal. Stereological measurements were made only on the low magnification (7,000x) micrographs.

Double-lattice stereology grids with lines 15 mm and 3.75 mm apart (Figure 3) were placed over the low power micrographs to obtain the stereological data by point counting. The larger grid size was used for myofilament, mitochondria, and nuclear volumes and the smaller grid for lipofuscin and myelin figure volumes. Approximately 25,000 total points were counted with the larger size grid and 400,000 points for the smaller grid for each group of the study. The volume percents from each block were treated as individual values for statistical purposes. Five blocks from one control animal were dropped from the study because it was impossible to adequately distinguish the different features on the micrographs. Values for the remaining blocks were analyzed per experimental group.

FIGURE 3. Longitudinal section of cardiac papillary muscle showing technique used for quantitative analysis. The print is overlaid with a thin sheet of transparent plastic inscribed with two rectangular grids. The larger grid (A) used for myofilament, mitochondria, and nuclear volumes was composed of lines 15 mm apart while the smaller grid (B) used for lipofuscin and myelin figures had lines 3.75 mm apart. (X7,000).

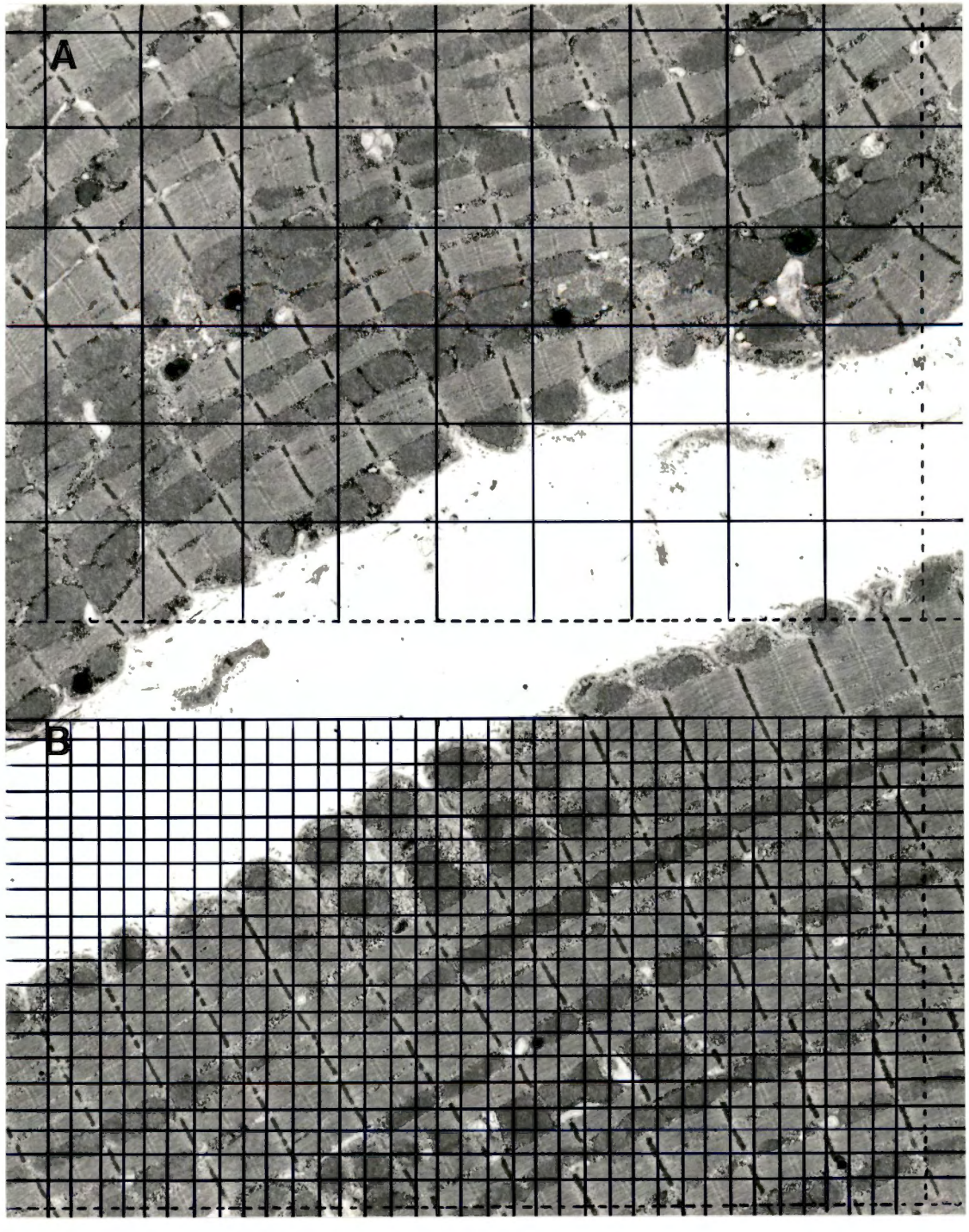

FIGURE 3

Statistical Analysis

An analysis of variance and Student's t-test were used to analyze all data except values for ALAD and TPP. Equality of variance was assured using Bartlett's test for equality of variances. A value of ($P < \text{or} = 0.05$) was taken as the acceptable limit of significance. ALAD and TPP data were analysed using Welch's test and Leven's variance test (33).

CHAPTER IV

RESULTS

Clinical Signs

All lead treated dogs developed clinical signs of lead poisoning while control dogs remained normal. Earliest signs included anorexia and weight loss followed by diarrhea and depression. Control dogs maintained or gained weight during the study, while dogs in both Pb groups lost weight as shown in Table C-II of Appendix C. Dehydration occurred in some treated animals. The decision to kill each animal was made when severe clinical signs were present, especially neurological involvement. Hyperesthesia, disorientation, and muscle fasiculations of the ears, eyelids, nose, forelimb and hind limb muscles were apparent on many treated dogs. In some dogs the main symptoms were anorexia and severe weight loss. Three animals had seizures (tonic-clonic) and ataxia; behavorial changes and other neurological signs were observed in others. In general, the gastrointestinal signs preceeded the neurological signs by one to two weeks.

A clear difference in the development of clinical signs between the Pb and the Pb + B_1 group was not observed. Each animal's condition appeared to deteriorate when the lead dosage was first increased at each dosage step, however, after a few days the dogs partially adjusted to the higher dose making it necessary to keep increasing the lead concentration. Each dog appeared to have a highly variable, individual tolerance to lead.

Hematological Parameters

The mean blood lead (BPb) level of the 15 dogs before treatment was 5.6 +/- 0.5 SEM µg/dl (deciliter). After lead treatment, BPb levels rose to 87 +/- 11.9 SEM µg/dl for the Pb treated group and 82 +/- 6.0 SEM µg/dl for the Pb + B_1 treated group. These levels are significantly ($p < .001$) higher than 7.8 +/- 1.7 SEM µg/dl, the BPb level of the control group found at the end of the study. The BPb levels of the Pb treated group and the Pb + B_1 treated groups are not different from each other. Table C-I of Appendix C shows blood lead concentrations and Tables C-III, C-IV, C-V, and C-VI shows original data for delta-aminolevulinic acid dehydratase (ALAD) activity, zinc protoporphyrin (ZPP) levels and tissue lead concentrations.

There were no significant differences among all groups for hemoglobin, total protein, total erythrocytes or total leukocytes before and after treatment. As seen in Table IV, values for thiamin pyrophosphate (TPP) appeared to increase significantly ($p < .05$) with lead treatment. The variances were found to be unequal by Leven's variance test so the data was analyzed by Welch's test (33) which corrects for unequal variences. TPP values for the Pb + B_1 group were significantly higher than those for Pb alone.

Delta-aminolevulinic acid dehydratase values are shown in Table V. The values decreased rapidly in both lead treatment groups to less than 25% of their original value within one week and to less than 10% by the end of the study. Since the variances were found to be unequal by Leven's variance test, the data was analyzed by Welch's test. A significant difference ($p < .001$) was found between the controls and

TABLE IV

ERYTHROCYTE THIAMIN PYROPHOSPHATE LEVELS[a]

Group	Animal #	Pretreatment	Posttreatment
Control			
	2	200	158
	6	141	160
	7	90	132
	12	170	150
	16	209	150
		162 (22)[b,c]	150 (5)[c]
Pb			
	5	106	225
	9	158	175
	11	113	366
	15	164	314
		135 (15)[c]	270 (43)[d]
Pb + B_1			
	4	119	645
	8	123	767
	10	135	750
	14	161	428
		135 (9)[c]	648 (78)[e]

[a] Expressed as ng/ml of PCV.

[b] Means +/- SEM given in ( ).

[c,d,e] Identical superscript indicates no significant difference ($p > 0.05$) while different superscript indicates significant difference ($p < 0.05$) between treatment groups.

TABLE V

ERYTHROCYTE DELTA-AMINOLEVULINIC ACID DEHYDRATASE VALUES[a]

Animal #	Pretreatment	Pb 1 week[b]	Pb 2 weeks	Final
Control				
2	282	*[c]	346	414
6	501	*[c]	497	396
7	237	*[c]	239	160
12	385	*[c]	299	237
16	366	331	289	144
	354 (46)[d,e]	331 (0)	334 (44)[e]	270 (57)[e]
Pb				
1	244	4	5	6
5	400	36	7	2
9	208	34	8	9
11	512	78	41	3
15	412	57	17	7
	355 (57)[e]	42 (12)	16 (7)[f]	5 (1)[f]
Pb + B_1				
3	439	70	8	14
4	718	130	7	10
8	226	45	6	10
10	275	96	56	25
14	425	67	3	7
	417 (86)[e]	82 (15)	16 (10)[f]	13 (3)[f]

[a] Expressed as nM PGB/ml RBC/hr

[b] Values were not analyzed for differences because of incomplete data.

[c] Data not collected

[d] Means +/- SEM given in ( ).

[e,f] Identical superscript indicates no significant difference ($p > 0.05$) while different superscript indicates significant difference ($p < 0.001$) between treatment groups.

both lead groups, however thiamin had no effect one way or the other on ALAD activity.

A trend for higher ZPP levels for the Pb and the Pb + B_1 groups was observed at 4 weeks (Table VI). These levels doubled in concentration by 6 to 8 weeks, the time of the final blood collection, and were significantly higher ($p < .05$) than pretreatment values.

Tissue Lead Analysis

The concentration of lead found in cardiac tissue (Table VII) increased significantly ($p < .01$) over controls in both the Pb and Pb + B_1 groups. There was no difference between the Pb and Pb + B_1 groups. Cardiac tissue contained 0.06 +/- 0.011 SEM mg/kg Pb for controls, 0.30 +/- 0.07 SEM mg/kg Pb for Pb treated and 0.37 +/- 0.077 SEM mg/kg for Pb + B_1. The tissue lead concentration (Table VII) in Pb treated and Pb + B_1 treated dogs was significantly higher ($p < .05$) than controls for liver, kidney, bone (femoral head), bone marrow, skeletal muscle, bile, brain stem, cerebral cortex, cerebellum, sciatic nerve, spinal cord, spleen, pancreas, testes, and lung tissue. There were no significant differences ($p > .05$) between tissue from Pb treated and Pb + B_1 treated animals. The original lead values are shown in Tables C-V and C-VI of Appendix C.

Physiological Function Tests

No significant differences ($p > .05$) in the hemodynamic responses were observed among the animals tested. However trends suggesting decreased cardiac function were observed in the Pb treated, but not in the Pb + B_1 treated dogs (Table VIII). The force of contraction as

TABLE VI

ERYTHROCYTE ZINC PROTOPORPHYRIN VALUES[a]

Animal #	Pretreatment	Pb 2 weeks	Pb 4 weeks	Final
Control				
2	0.8	0.6	0.6	0.8
6	1.4	1.1	0.9	1.5
7	0.8	0.8	1.1	1.6
12	1.6	1.4	1.3	1.3
16	0.8	0.5	0.9	0.6
	1.1 (0.2)[c,d]	0.9 (0.2)[d]	1.0 (0.1)[d]	1.2 (0.2)[d]
Pb				
1	1.6	1.9	*[b]	1.9
5	1.1	1.5	1.4	3.1
9	0.6	1.2	1.6	1.5
11	0.9	0.8	1.1	1.9
15	0.9	0.6	1.1	1.4
	1.0 (0.2)[d]	1.2 (0.2)[d]	1.3 (0.1)[d]	2.0 (0.3)[e]
Pb + B_1				
3	0.4	1.3	1.4	2.3
4	1.5	1.9	1.7	3.2
8	0.7	1.5	1.9	2.5
10	0.9	8.9	8.0	7.1
14	1.6	1.4	1.9	2.9
	1.0 (0.2)[d]	3.0 (1.5)[d]	3.0 (2.0)[d]	3.6 (0.9)[e]

[a] Expressed as ug ZPP/Gm Hb

[b] Data was not collected

[c] Means +/- SEM given in ( ).

[d,e] Identical superscript indicates no significant difference ($p > 0.05$) while different superscript indicates significant difference ($p < 0.05$) between treatment groups.

TABLE VII

CONCENTRATION OF LEAD IN CANINE TISSUE SAMPLES[a]

Tissue	Control	Pb	Pb + B_1
Heart	0.06 (0.01)[b]	0.30 (0.07)[c]	0.37 (0.08)[c]
Vastus Lateralis Muscle	0.05 (0.01)[b]	0.27 (0.02)[c]	0.29 (0.08)[c]
Biceps Muscle	0.04 (0.01)[b]	0.24 (0.03)[c]	0.33 (0.07)[c]
Liver	0.72 (0.30)[b]	48.00 (6.40)[c]	49.41 (9.99)[c]
Kidney	0.41 (0.16)[b]	25.52 (5.39)[c]	29.46 (8.08)[c]
Bone (Femoral Head)	11.55 (3.19)[b]	74.59 (7.01)[c]	94.72 (6.50)[c]
Bone Marrow	1.02 (0.30)[b]	3.46 (0.31)[c]	8.26 (2.13)[c]
Bile	0.12 (0.03)[b]	8.22 (1.45)[c]	6.88 (2.75)[c]
Brain Stem	0.10 (0.01)[b]	1.10 (0.10)[c]	0.96 (0.13)[c]
Cerebral Cortex	0.09 (0.02)[b]	1.64 (0.51)[c]	1.31 (0.09)[c]
Cerebellum	0.17 (0.04)[b]	0.93 (0.08)[c]	0.75 (0.10)[c]
Nerve	0.18 (0.12)[b]	0.88 (0.10)[c]	0.94 (0.17)[c]
Spinal Cord	0.10 (0.02)[b]	0.76 (0.05)[c]	0.56 (0.14)[c]
Spleen	0.16 (0.04)[b]	7.43 (1.03)[c]	7.41 (1.50)[c]
Pancreas	0.24 (0.10)[b]	2.10 (0.15)[c]	1.88 (0.22)[c]
Testes	0.08 (0.02)[b]	0.68 (0.06)[c]	0.55 (0.11)[c]
Lung	0.11 (0.03)[b]	1.24 (0.05)[c]	1.15 (0.09)[c]

[a] Expressed as mg/kg Pb with means +/- SEM given in ( ).

[b,c,] Identical superscript indicates no significant difference ($p > 0.05$) while different superscript indicates significant difference ($p < 0.05$) between treatment groups.

TABLE VIII

CANINE VENTRICULAR HEMODYNAMIC RESPONSE MEASURED BEFORE AND AFTER EXPOSURE TO LEAD AND LEAD PLUS THIAMIN[a,b]

Hemodynamic Parameter	Treatment Group	Time of Measurement	
		Pretreatment	Posttreatment
dP/dT mmHg/sec	Control	2880 (320)	3100 (245)
	Pb	3550 (635)	2575 (674)
	Pb + B_1	3620 (361)	3600 (828)
Peak Ventricular Pressure (mm Hg)	Control	140 (9)	184 (17)
	Pb	158 (9)	116 (15)
	Pb + B_1	121 (7)	116 (19)
Heart Rate (Beats Per Minute)	Control	162 (17)	174 (14)
	Pb	176 (14)	169 (19)
	Pb + B_1	174 (4)	162 (13)
Ventricular Extrasystolic beats/minute during Norepinephrine infusion (4 ug/kg/min)	Control	69 (17)	57 (15)
	Pb	61 (32)	18 (18)
	Pb + B_1	19 (8)	10 (9)

[a] Means +/- SEM given in ( ).

[b] No Significant differences ($p > .05$) are shown, however trends can be observed.

measured by the first derivative of ventricular pressure (Dp/dt at 50 mm Hg developed isovolumic pressure) was decreased in the Pb treated animals. The peak ventricular pressure also declined for dogs in the Pb treated group. Differences were not observed in the resting heart rate or in the number of extrasystolic beats/2-minute intervals obtained as the dogs were tested for susceptability to the development of ectopic electrical activity with norepinephrine.

Stereological Analysis

The volumetric data obtained from a stereological analysis of myocardial cells from the left ventral papillary muscle is shown in Table IX. In dogs treated with Pb alone, the volume of the cell occupied by myofilaments increased significantly by 3.2% over the control group. In dogs treated with Pb and B_1, there was no significant increase or decrease in myofilament volume. The volume occupied by mitochondria decreased significantly in dogs from both the Pb and Pb + B_1 groups as compared to controls. There was no significant difference between the two experimental groups. Nuclear volume was unchanged with either Pb or Pb + Pb_1 treatment when compared to controls. The cell volume occupied by intracellular space and remaining cellular components was greater for the Pb + B_1 group than the control or Pb group.

The mitochondria to myofilament ratio, an index frequently used to characterize hypertrophic or other changes in the myocardium, was significantly decreased in dogs from the Pb group, but not in dogs from the Pb + B_1 group. The ratio in the Pb group was also

TABLE IX

COMPOSITION OF VENTRAL PAPILLARY MUSCLE FROM CANINE LEFT VENTRICLES: VOLUME RELATIONSHIPS[a]

	Control	Pb	Pb + B_1
Volume %:			
Myofilaments	55.6 (0.6)[b]	58.8 (0.6)[c]	55.1 (0.7)[b]
Mitochondria	23.5 (0.4)[b]	21.4 (0.4)[c]	22.0 (0.4)[c]
Nucleus	1.3 (0.2)[b]	1.2 (0.2)[b]	1.3 (0.1)[b]
Other	19.6 (0.7)[b]	18.6 (0.7)[b]	21.6 (0.7)[c]
Mitochondrial volume/myofilament volume:	0.425 (0.008)[b]	0.366 (0.007)[c]	0.404 (0.009)[b]

[a] Means +/- SEM given in ( ).

[b,c,d] Identical superscript indicates no significant difference ($p > 0.05$) while different superscript indicates significant difference ($p < 0.01$) between treatment groups.

significantly lower than the Pb + B_1 group. Ratios are listed in Table IX.

Volume percents were determined for lipofuscin pigment and myelin figures, but even with transformation of the data, the variances were too unequal for meaningful statistical evaluation. Even so, lipofuscin volumes were 0.16% for controls; 0.15% for Pb; and 0.12% for Pb + B_1 and myelin figure volumes were 0.042% for controls; 0.026% for Pb; 0.016% for Pb + B_1. Original values for the stereological analysis are shown in Tables C-VII, C-VIII, and C-IX of Appendix C.

Morphological Results

The appearance of myocardium from control dogs was essentially the same as myocardium from the Pb and the Pb + B_1 dogs. The following descriptions apply to all three groups unless otherwise specified.

Nuclei had prominent nucleoli, uniformly distributed chromatin granules and thin condensation rims of peripheral heterochromatin. No nuclear damage was observed. Nuclear inclusions found in lead poisoned kidney tubule cells were not seen in myocyte nuclei.

The vast majority of cells had intact sarcolemma closely applied to the myofilaments and mitochondria (Figure 2, p 21 and Figures 4,5). Cellular edema while rarely evident, was occasionally observed in control and both lead treated groups (Figures 6,7). Mitochondria found in edematous tissue usually appeared normal. Contraction bands and widening of intermembranous spaces of the intercalated discs were not evident.

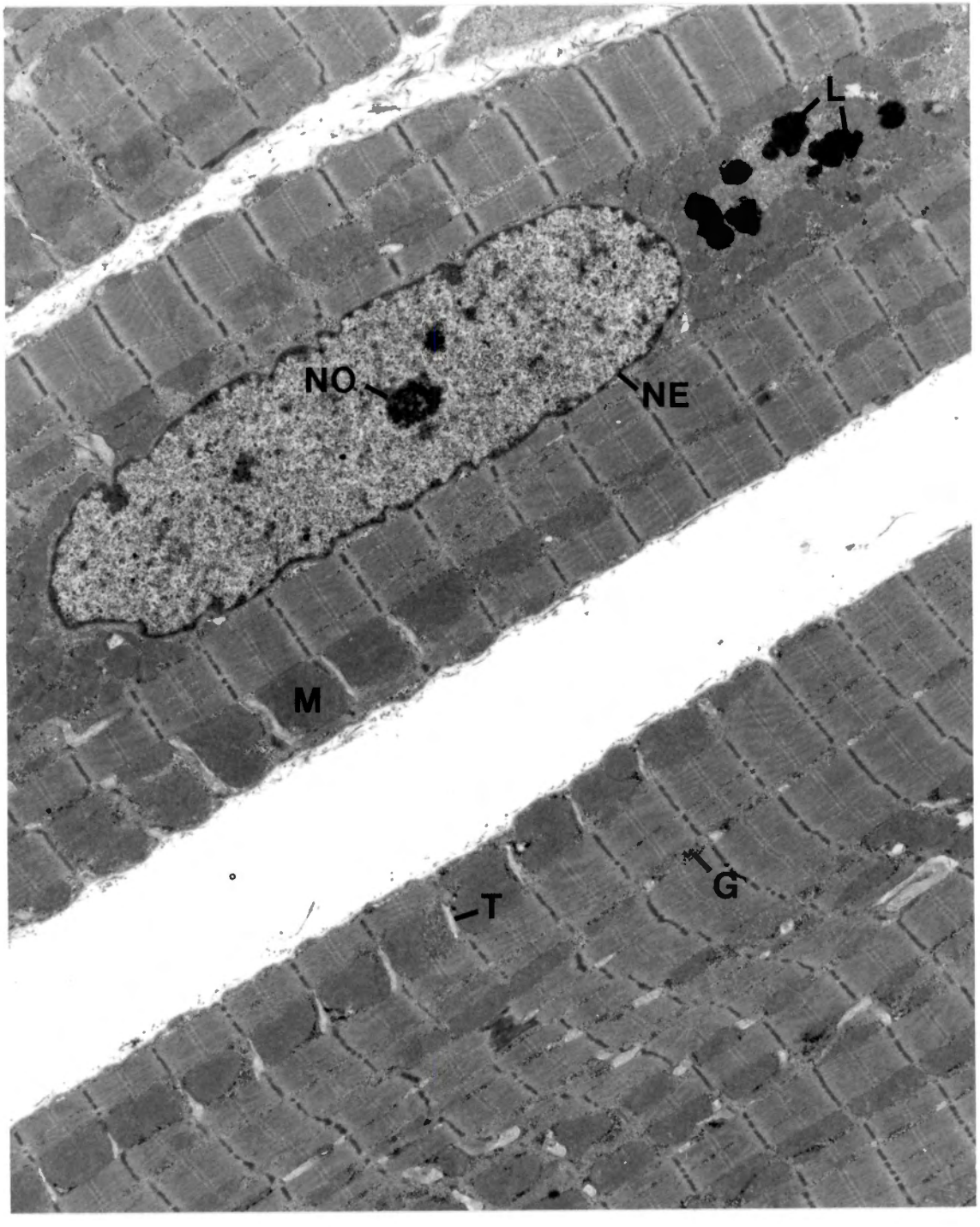

FIGURE 4. Cardiac papillary muscle from a Pb treated dog. Nuclear envelope (NE), nucleolus (NO), mitochondria (M), lipofuscin (L), glycogen (G), T tubule (T). (X7,000).

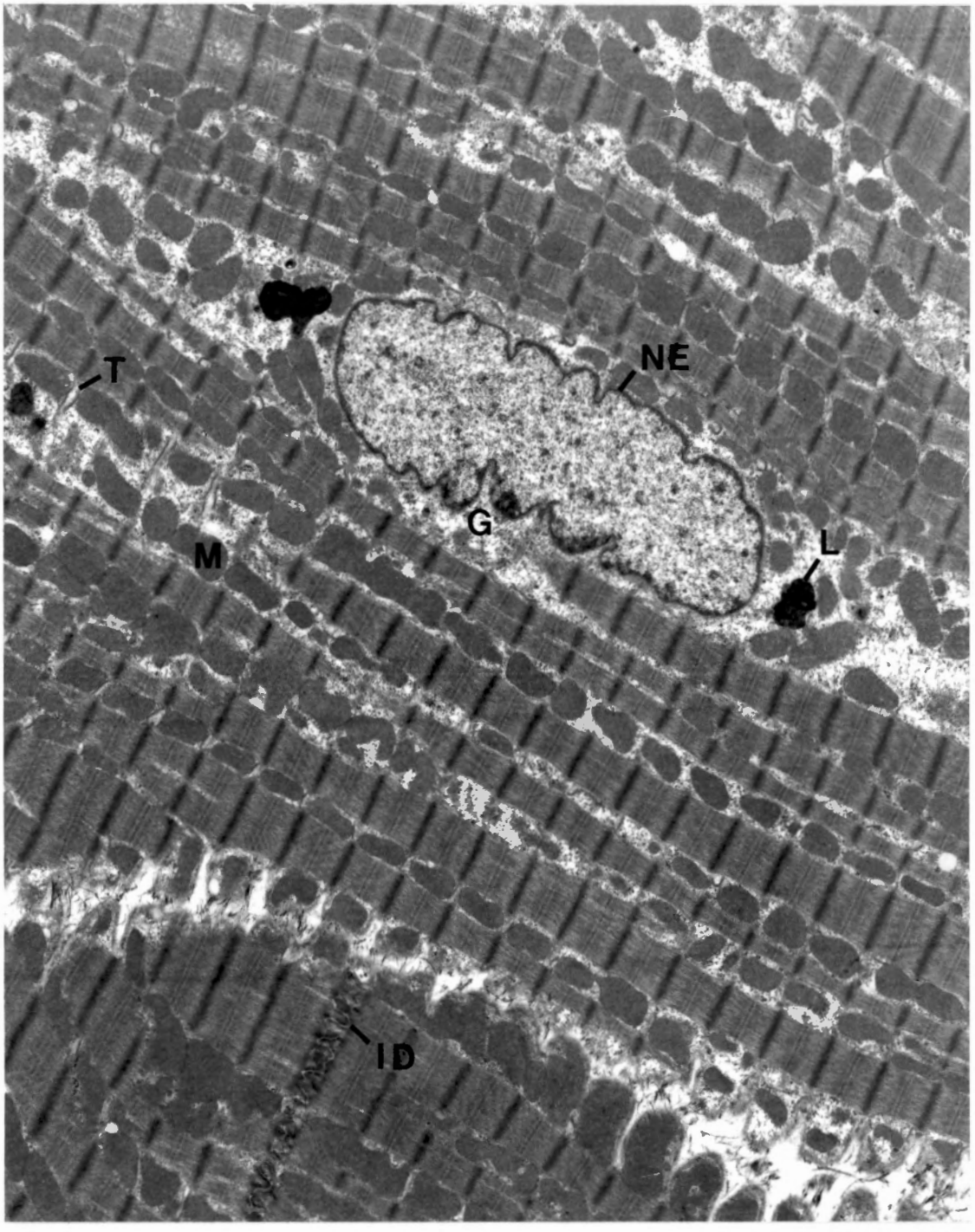

FIGURE 5. Cardiac papillary muscle from a Pb + B_1 treated dog. Nuclear envelope (NE), mitochondria (M), lipofuscin (L), glycogen (G), T tubule (T), Intercalated disc (ID). (X7,000).

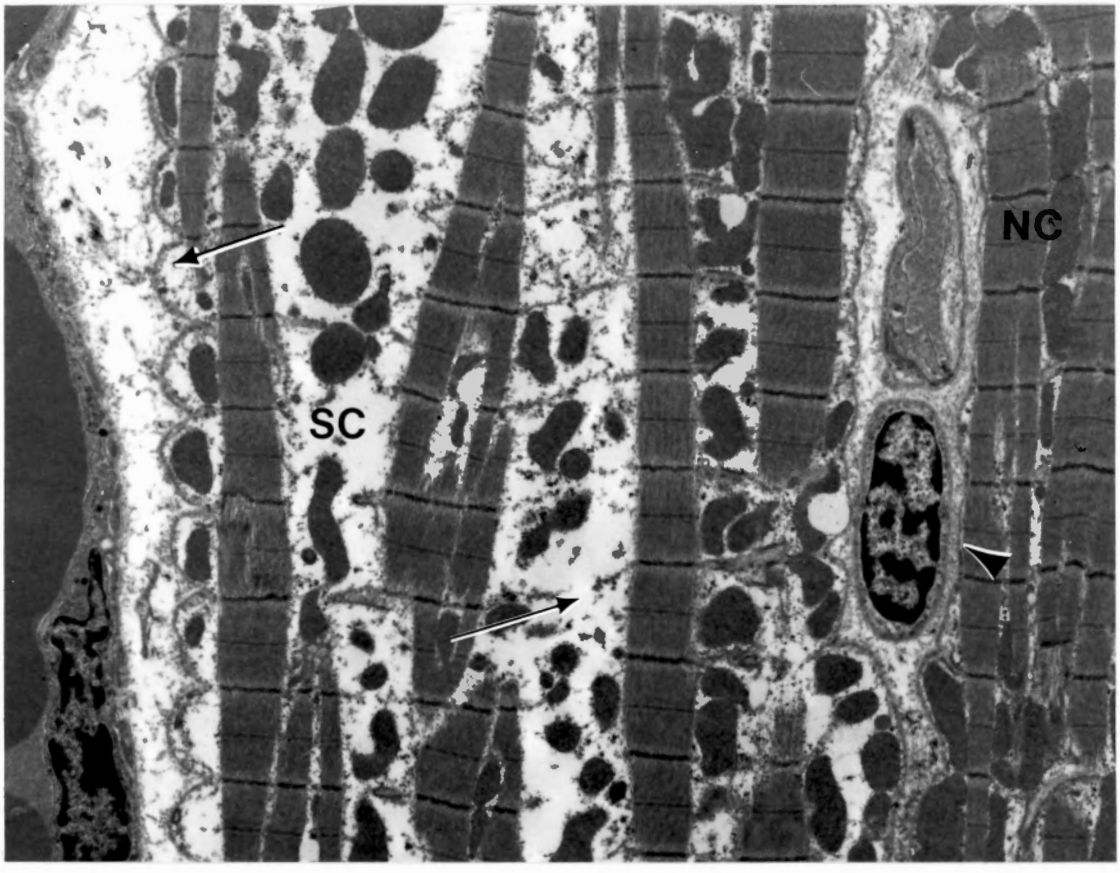

FIGURE 6. Intracellular edema of the papillary myocardium from a control dog. A swollen cell (SC) with clear spaces (arrows) and a sarcolemna lifted away from the myofilaments and mitochondria is found adjacent to a normal appearing cell (NC). The normal cell has a tightly apposed sarcolemna (arrowhead). (X7,000).

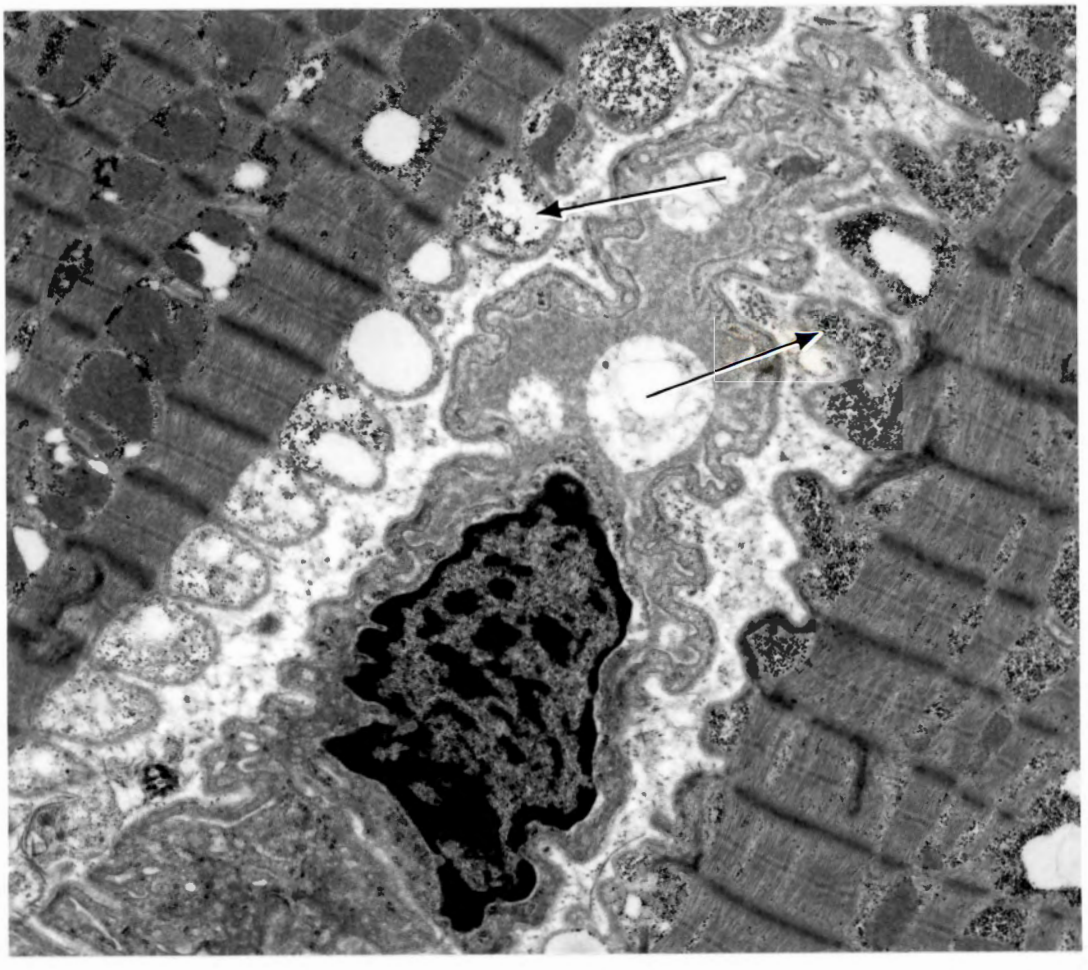

FIGURE 7. Intracellular edema of the papillary myocardium from a Pb treated dog. The sarcolemna is lifted off the myofilaments (arrows), but unlike figure 6, the myofilaments are not separated by clear areas, but remain tightly apposed to the mitochondria and each other. (X7,000).

The appearance of mitochondria was the same in all treatment groups (Figure 2, p 21 and Figures 4,5,8). Mitochondria, regularly spaced between the myofilaments and in the perinuclear area, contained well formed cristae with electron dense matrices. Giant mitochondria were rarely seen. Swollen mitochondria, while infrequently enountered, were surrounded by normal appearing mitochondria (Figure 9).

Areas of fibrinolysis were only rarely encountered in the myofilament mass. Z lines were prominent, in register across the myocytes, and often associated with T tubules. Lipofuscin, commonly located near the nucleus, was found in most of the blocks examined. Myelin figures, circular swirls of membrane were less common. Specific changes were not seen in lysosomes, lipids or the sarcoplasmic reticulum. Moderate amounts of glycogen were present in sarcoplasm near the nucleus and scattered between the myofilaments. Blood vessel damage or large areas of interstitial fibrosis was not apparent.

FIGURE 8. High power magnification of mitochondria from a Pb treated dog. Moderate amounts of glycogen (G) are interspersed between myofilaments (F) and mitochondria (M). Mitochondria contain well formed cristae (arrow) and electron dense matrices. (X65,000).

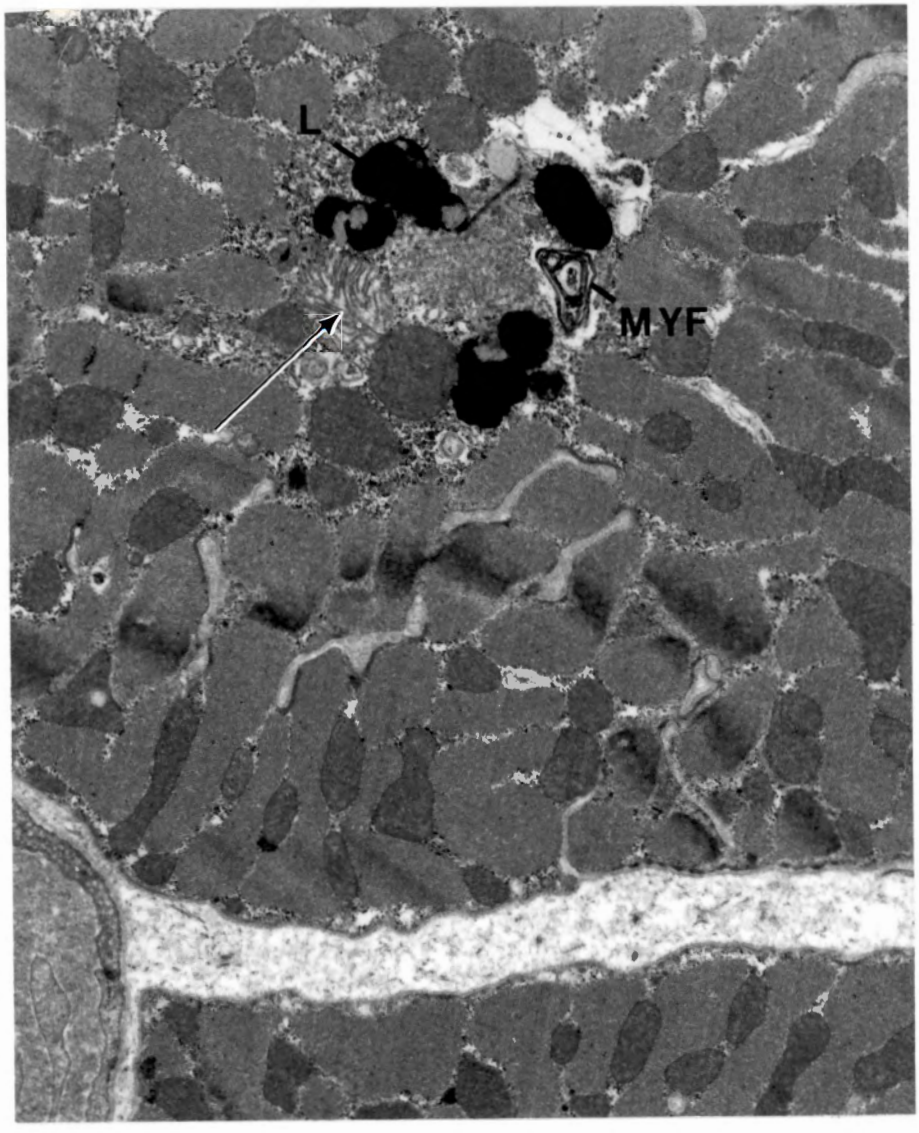

FIGURE 9. Mitochondria from the papillary muscle of a Pb treated dog. While one mitochondrion is swollen (arrow), others surrounding it appear normal with electron dense matrices. Lipofuscin deposits (L) are routinely seen and myelin figures (MYF) are noticed occasionally. (X10,800).

CHAPTER V

DISCUSSION

Stereological and Morphological Analysis

All previous morphological studies on the effect of lead on cardiac tissue have been qualitative in nature. This study represents the first quantitative investigation. Relative measurements using stereological techniques compared the volume fractions of cellular components of the three groups under study: control, Pb and Pb + B_1. The control values reported for mitochondrial and myofilament volumes are consistent with previously published reports on canine left ventricle myocardium (50,88).

The major finding of the stereological analysis was the statistically significant increase of 3.2% in the volume occupied by myofilaments in animals from the Pb only group and the significant decrease in the volume of mitochondria observed in animals from both the Pb and Pb + B_1 group. This volume change is similar to the reported response of myocardium in hypertrophy. A myofilament increase of 7% and a mitochondrial decrease of 3% was observed by Page and McCallister (98) and Page et al. (100) in studies of experimentally produced hypertension in rats. In human cardiac tissue, patients with pathologically hypertrophied left ventricles had a 10% increase in myofilament volume over non-hypertrophied hearts (41). In addition, the mitochondrial volume was about 8% below

non-hypertrophied hearts. Fleischer and Warmuth (41) found their result "surprising because in qualitative investigations mitochondria accumulate in large areas between the myofibrils and point to an increase of the mitochondrial part of the cell." The results of their surgical biopsy studies contradicted their previous assumptions on mitochondrial increases. Similar unspecific ultrastructural alterations occur in most cardiac diseases and this study also demonstrates a possible way to distinguish between different cardiac diseases by using morphometric methods to quantify cellular components.

The ratio of mitochondria to myofilaments changes in hypertrophy. With prolonged hypertrophy, the volume ratio of mitochondria to myofilament mass decreases progressively and may lead to a deficient energy supply and eventually to a compromise of contractility in the heart (2). The present study showed a trend toward decreased contractility of the heart as measured by declining values for Dp/dt mmHg/sec in animals from the Pb treated group. The trend for lower peak ventricular pressure in Pb treated dogs is consistent with a decrease in contractility. These effects were not observed in control or Pb + B_1 treated animals. In hypertrophy, the diffusion distance increases which could lead to a decrease in contractility. Stereological analysis revealed a statistically significant decrease in the mitochondria/myofilament volume ratio in dogs of the Pb only group, but not in dogs from the Pb + B_1 group. The lack of both a mitochondria/myofilament ratio change and myocardial functional change indicates a possible protective effect of thiamin on the mitochondria

or less of a compensatory need of the myocyte to increase the myofilament volume.

Electron microscopic observations alone showed no morphological differences in mitochondria from different treatment groups; quantitative measurements were needed to observe the differences in chronic lead poisoning in adult animals. While mitochondrial space decreased, the functional condition of the remaining mitochondria was not known. Lead has been shown to accumulate in mitochondria (7,94,111) and adversely affect them (16,54,91). The decrease in mitochondrial volume in the present study supports this premise. The decrease in mitochondrial volume was smaller in this study than is generally seen in ischemia (88) and was not accompanied by a decrease in myofilament volume, a finding that would have indicated cellular swelling. The morphological analysis only rarely found cellular edema; the sarcolemna in most cases was tightly applied to the myofilaments or the mitochondria. The stereological analysis confirmed a lack of cellular edema.

Lead poisoning has been shown to cause morphological changes in cardiac tissue (4,73,74,91,92). While no morphological damage was observed in the present study of chronic, but lethal lead poisoning in dogs, this study involved adult animals. Kline (74) described chronic myocarditis in children aged 18 to 26 months who died of lead poisoning. Mitochondrial changes, including swelling, loss of regular spacing and orientation and abnormal clumping and rarefaction of the matrix were reported in 20 gm mice (73), 330 gm, 6 week old rats (4), 200 gm rats (92), and 250 gm rats (91). These studies involved young,

growing children and animals and would be expected to show greater damage to developing systems including the cardiovascular system. Children are at greatest risk of nonoccupational lead poisoning (55) because of their increased sensitivity, while adults who work with lead products and by-products are at continual risk of chronic intoxication. Very few animal studies have concentrated on adults as models for human adult lead poisoning.

Lipofuscin and myelin figure volume percents were determined, but the raw data did not indicate increases with Pb or Pb + B_1 treatment, however the results could not be analyzed statistically because of unequal variances even after transformation of the data. Using point counting techniques, 400,000 points were counted to determine the volume percents of lipofuscin and myelin figures. It was determined from previous test counts that at least 249,000 points (assuming a 5% standard error) would be needed to determine a rare event of 0.16% for lipofuscin, so the number of points counted was sufficient. For the myelin figure determinations, 240,000 points (assuming a 10% standard error) were needed to measure the 0.042% obtained for the control animals and 385,000 points for the 0.026% in the Pb group. A volume of 0.016% was measured for animals of the Pb + B_1 group so 625,000 points would have been needed to accurately determine myelin figure volume. Since sufficient points were counted in most cases, the unequal variances were unexplained. The reason for the unequal variances is likely related to the previous health of the dogs. The animals were quarantined for at least two weeks, but previous health records were unavailable. Previous viral or bacterial

infections could have affected the morphological picture of the myocardium as a whole in addition to the specific affect on myelin figures and lipofuscin. The dog's ages, while similar, were not documented and therefore could have contributed to the variation, especially the lipofuscin volume which is known to increase with age or with atrophic diseases of the heart (82).

Functional Changes

The results obtained with the physiological function tests can be correlated with the stereological and morphological results. Significant differences ($p > .05$) were not found, however a downward trend in the force of contractility as measured by Dp/dt mmHg/sec and in peak ventricular pressure was observed only in dogs of the Pb treated group. Lead poisoning has been shown to increase the suceptibility of the myocardium to extrasystolic beats when stimulated by epinephrine (61,62), however the animals in these studies were young, developing rats and this effect could have resulted from previous exposure of the developing nervous system to lead. Changes in extrasystolic beats were not observed in the present study.

The morphological and functional changes which occurred in the heart although not major, were found to exist. This might be important in the light of White and McLeod's (127) work which showed some evidence for the existence of a latent effect of lead on certain body systems. They used distemper virus to experimentally infect dogs who were previously exposed to lead and then assessed the response of the body to the infection. An altered response of the whole body or

certain systems to other disease processes might result from a previous exposure to lead.

Clinical Picture

Clinically, the dogs with either Pb or Pb + B_1 treatment showed severe signs of lead poisoning. Thiamin had little effect on the clinical picture, in contrast to the results of Bratton et al. (13,14) where calves treated with thiamin in addition to lead showed no clinical signs. In their work, four of five calves treated with lead alone showed signs of lead intoxication, including the death of two calves. Approximately the same clinical picture was reported in a followup study by Mollenhauer et al. (90) where some lead poisoned, untreated calves died in contrast to EDTA treated or thiamin treated calves which remained in good general health. Results by Louis-Ferdinand et al. (86) in lead poisoned rats given thiamin (T) suggest that "acute Pb lethality is not affected by concomitant T administration."

Hematological Parameters

General hematological parameter were unchanged with Pb or Pb + B_1 treatment. ALAD, ZPP and TPP levels were affected. The decrease in ALAD activity was rapid, dropping to less than 25% by one week, irrespective of thiamin treatment. This agrees with results by Bratton et al. (13) in calves.

Only a small rise was noted in ZPP levels in the lead poisoned groups. ZPP levels rise significantly in cattle, sheep, and horses poisoned by lead (11,80). A ZPP increase from 2-3 to 6-7 µg ZPP/Gm Hg

occurred as early as one week after lead ingestion in a study of young calves (134) and continued to rise to 100 µg ZPP/Gm Hb by the eighth week of lead treatment. The ZPP levels for the Pb and Pb + B_1 treated dogs in the present study while not significantly increased over controls at 4 weeks, doubled in concentration by 6 to 8 weeks, significantly higher than pretreatment levels ($p < .05$). In normal and lead poisoned humans, ZPP comprises 90% of the total protoporphyrins in blood (37). In cattle, this percent has been reported as low as 66% (48). Apparently a significant formation of ZPP with lead poisoning does not occur in canine erythrocytes, however further investigation is needed. One Pb + B_1 treated dog had normal pretreatment ZPP levels which rose to 8 times normal after one week and remained at that level throughout the study. Karacic et al. (68) have reported false positive increases of ZPP due to bilirubin and this provides one possible explanation of this unusual increase.

Lead and Thiamin Interactions

Tissue and blood lead levels in this study do not indicate a protective effect of thiamin in lead poisoning. Earlier calf studies by Bratton et al. (13,14) pointed to a protective effect of thiamin; the tissue lead levels in the kidney, liver and brain of lead and thiamin treated calves were lower than the lead-only treated animals. These studies used very young calves on a milk replacer diet. The age difference may be the main reason for the difference between the two studies, however species differences may also exist. Louis-Ferdinand et al. (86) also reported 26 to 37% lower blood, brain, bone, kidney

and liver lead levels in weanling rats receiving thiamin in addition to lead. Thiamin administration did not alter brain levels of lead in rats (131).

A study by Woolley-Efigenio et al. (131) in young developing rats evaluated the neurotoxic effects of lead related to the thiamin status of the animals. Lead was administered in drinking water in doses which did not cause a decrease in body growth, but did produce an anticonvulsant effect on the maximal electroshock seizure (MES) patterns. Thiamin administered subcutaneously reversed most of the effects on the MES. While this effect was maximal during growth, it decreased as the rats reached adulthood (130).

In studies using thiamin deficient diets and lead, there are no clear cut conclusions to be drawn. Studies using thiamin deficient diets may differ substantially from those using an excess of thiamin to affect the lead deposition in animals. Woolley-Efigenio et al. (131) studied rats on thiamin deficient diets treated with lead. Initially the low thiamin plus lead group fell behind the high thiamin plus lead group in body growth rate. At the end of the experiment, thiamin appeared to be the determining factor in animal weight; low thiamin, lower weight. In addition, "Lead exposure initially had an anticonvulsant effect in the high thiamin group. Low thiamin itself had a convulsant effect which was worsened by lead." Their results "indicate that low dietary thiamin levels may exacerbate the toxicity of lead, and that high thiamin levels may ameliorate it."

The interaction of lead and thiamin is not clear. While Bratton et al. (14) postulated that less lead was absorbed in thiamin treated

calves, subsequent studies in rats (109) showed that thiamin facilitated absorption of a single dose of lead from the gastro-intestinal tract and increased the amount of lead initially taken up by body tissues. Their results (109) indicate that "Thiamin may also promote more rapid release of lead from tissues." While the investigators postulated the formation of a lead-thiamin complex, "preventing prolonged binding of lead to tissues . . . metal-thiamin complexes have not been demonstrated in vivo" (109). Rats in a thiamin-depleted group inititally absorbed less lead than the control group, however by 72 hours this trend was reversed. In this study using rats, very little lead (less than 0.05% of the dose) was excreted in the urine. This is in contrast to the investigation by Louis-Ferdinand et al. (86) which found that lead and thiamin administered to adult mice increased by 70% the urinary output of lead without altering the 24 hour fecal excretion of lead. Results by Louis-Ferdinand et al. (86) also indicated that thiamin increases blood lead initially possibly by altering the soft tissue lead distribution. They stated that "the tissue Pb lowering effect of T administered concomitantly is not the result of decreased Pb absorption."

Erythrocyte TPP levels were found to increase in dogs of the Pb treated group. The Pb + B_1 treated dogs had even higher levels of TPP since these animals were injected daily with thiamin. Thiamin pyrophosphate is the active coenzyme form of vitamin B_1. The possibility exists that lead and thiamin interact in such a way that lead forces the thiamin out of the tissues. The formation of a

lead-thiamin complex must still be considered. Bratton et al. (14) found the erythrocyte transketolase activity unaltered in lead and lead plus thiamin treated calves. Transketolase activity was also unaltered in lead poisoned cattle (85) and rats (130). In contrast, Tokarski and Reio (118) found a decrease of 5 to 40% in the activity of erythrocyte transketolase in rats given subcutaneous injections of lead acetate as well as a decrease in liver thiamin. Additional studies are needed to clarify the interaction of lead and thiamin within the body.

LIST OF REFERENCES

LIST OF REFERENCES

1. Albahary C: Lead and hemopoiesis: The mechanism and consequences of the erythropathy of occupational lead poisoning. Am J Medicine 52:367-378, 1972.

2. Anversa P, Loud AV, Giacomelli F, Wiener J: Absolute morphometric study of myocardial hypertrophy in experimental hypertension. II Ultrastructure of myocytes and interstitium. Lab Invest 38:597-609, 1978.

3. Aposhian HV: DMSA and DMPS - Water soluble antidotes for heavy metal poisoning. Ann Rev Pharmacol Toxicol 23:193-215, 1983.

4. Asokan SK: Experimental lead cardiomyopathy: myocardial structural changes in rats given small amounts of lead. J Lab Clin Med 84:20-25, 1974.

5. Balazs T, Ferrans VJ: Cardiac lesions induced by chemicals. Environmental Health Perspectives 26:181-191, 1978.

6. Bartik M, Piskac A: Veterinary Toxicology, in: Developments in Animal and Veterinary Sciences. Vol. 7. Amsterdam, Elsevier Scientific Publishing Co, 1981, pp 108-118.

7. Barltrop D, Barrett AJ, Dingle JT: Subcellular distribution of lead in the rat. J Lab Clin Med 77:705-712, 1971.

8. Blumberg WE, Eisinger J, Lamola AA, Zuckerman DM: Zinc protoporphyrin level in blood determined by a portable hematofluorometer: a screening device for lead poisoning. J Lab Clin Med 89:712-723, 1977.

9. Bozner A, Meessen H: Die freinstruktur des herzmuskels der ratte nach einmaligem und nach wiederholtem schwimmtraining. Virchows Arch Abt B Zellpath 3:248-269, 1969.

10. Bratton GR: Personal communication. July, 1985.

11. Bratton GR, Childress MJ: Hematofluorometric determination of zinc protoporphyrin: an aid to diagnosis of lead poisoning in ruminants. Abstract 62nd Conf Res Workers An Dis p 6, 1981.

12. Bratton GR, Zmudzki J: Ca-EDTA and Vitamin B_1 treatment in lead poisoned cattle. Conference of Research Workers in Animal Disease. 65th Annual Meeting, Chicago, IL, 1984. (Abstract)

13. Bratton GR, Zmudzki J, Bell MC, Warnock LC: Thiamin (Vitamin B_1) Effects on lead intoxication and deposition of lead in tissues: therapeutic potential. Toxicol Appl Pharmacol 59:164-172, 1981.

14. Bratton GR, Zmudzki J, Kincaid N, Joyce J: Thiamin as treatment of lead poisoning in ruminants. Mod Vet Pract 62:441-446, 1981.

15. Burch HB, Siegel AL: Improved method for measurement of delta-aminolevulinic acid dehydratase activity of human erythrocytes. Clin Chem 17:1038-1041, 1971.

16. Cardona E, Lessler MA, Brierley GP: Mitochondrial oxidative phosphorylation: Interaction of lead and inorganic phosphate. Proc Soc Exp Biol Med 136:300-304, 1971.

17. Carlson BL, Nielsen SW: Influence of dietary calcium on lead poisoning in mallard ducks (Anas playrynchos). Am J Vet Res 46:276-282, 1985.

18. Center for Disease Control, a statement: Preventing lead poisoning in young children. J Pediatr 93:709-720, 1978.

19. Chakrabarti SK, Brodeur J, Tardif R: Fluorometric determination of delta-aminolevulinic dehydratase activity in hyman erythrocytes as an index to lead exposure. Clin Chem 21:1783-1787, 1975.

20. Chisholm JJ Jr: Treatment of lead poisoning. Mod Treat 8:593-611, 1971.

21. Chisolm JJ Jr: Heme metabolites in blood and urine in relation to lead toxicity and their determination. Adv Clin Chem 20:225, 1978.

22. Chisolm JJ Jr: Poisoning from heavy metals (mercury, lead and cadmium). Pediatric Ann 9:458-468, 1980.

23. Chisolm JJ Jr: Management of increased lead absorption and lead poisoning in children. N Engl J Med 289:1016-1018, 1973.

24. Choie DD, Richter GW: Lead poisoning: rapid formation of intranuclear inclusions. Science 177:1194, 1972.

25. Cikrt M, Bencko V: Hygienic-toxicological aspects of exposure to lead. A critical review. J Hyg Epid Micro Epid 26:343-357, 1982.

26. Cullen MR, Robins JM, Eskenazi B: Adult inorganic lead intoxication. Medicine 62:221-247, 1983.

27. Currie MG, Geller DM, Cole BR, Boylan JG, Yusheng W, Holmberg SW, Needleman P: Bioactive cardiac substances: potent vasorelaxant activity in mammalian atria. Science 221:71-73, 1983.

28. Datta BU, Silver MD: Cardiomegaly in chronic anemia in rats. Lab Invest 32:503-514, 1975.

29. David H: Quantitative ultrastructural data of animal and human cells. Stuttgart, Gustav Fisher Verlag, 1977, pp 395-408.

30. de Bold AJ, Borenstein HB, Veress AT, Sonnenberg H: A rapid and potent natriuretic response to intravenous injection of atrial myocardial extract in rats. Life Sci 28:89-94, 1981.

31. de Bold AJ, Flynn TG: Cardionatrin I - A novel heart peptide with potent diuretic and natriuretic properties. Life Sci 33:297-302, 1983.

32. De Hoff RT, Bousquet: Estimation of the size distribution of triaxial ellipsoidal particles from the distribution of linear intercepts. J Microscopy 92:119, 1970.

33. Dixon WJ: BMDP Statistical Software. Berkeley, University of California Press, 1983.

34. Eisenberg B: Skeletal muscle fibers: stereology applied to anisotropic and periodic structures in Weibel ER (ed):Stereological Methods. Vol 1. Practical Method for Biological Morphometry. New York, Academic Press, 1979, pp 274-284.

35. Eisenberg BR, Kuda AM, Peter JB: Stereological analysis of mammalian skeletal muscle. I. Soleus muscle of the adult guinea pig. J Cell Biol 60:732, 1974.

36. Eisinger J: Biochemistry and measurement of environmental lead intoxication. Quarterly Reviews of Biophysics II. 4:439-466, 1978.

37. Eisinger J, Blumberg WE, Fischbein A, Lilis R, Selikoff IJ: Zinc protoporphyrin in blood as a biological indicator of chronic lead intoxication. J Environ Path Toxicol 1:897-910, 1978.

38. Elias H, Hennig A, Schwartz DE: Stereology: Applications to biomedical research. Physiological Reviews 51:158-200, 1971.

39. Elias H, Hyde D: An elementary introduction to stereology (quantitative microscopy). Am J Anat 159:412-446, 1980.

40. Ferrans VJ, Hibbs RG, Walsh JJ, Burch GE: Histochemical and electron microscopical studies on the cardiac necroses produced by sympathomimetic agents. Ann New York Acad Sci 156:309-332, 1969.

41. Fleischer M, Warmuth H: Ultrastructural morphometric analysis on normal loaded and on hypertrophied human myocardial left ventricles, in Bolte H-D, (ed): Myocardial Biopsy. Berlin, Springer-Verlag, 1980, pp 49-52

42. Freeman R: Reversible myocarditis due to chronic lead poisoning in childhood. Arch Dis Child 40:389-393, 1965.

43. Friedheim E, Corvi C, Wakker CH: Meso-dimercaptosuccinic acid a chelating agent for the treatment of mercury and lead poisoning. J Pharm Pharmacaol 28:711-712, 1976.

44. Friedheim E, Graziano JH, Popovac D, Dragovic D, Kaul B: Treatment of lead poisoning by 2,3-dimercaptosuccinic acid. Lancet 2:1234-1236, 1978.

45. Friedman I, Moravec J, Reichart E, Hatt PJ: Subacute myocardial hypoxia in the rat. An electron microscopic study of the left ventricular myocardium. J Mol Cell Cardiol 5:125-132, 1973.

46. Ganote CE, Worstell J, Lannotti JP, Kaltenback JP: Cellular swelling and irreversible myocardial injury. Am J Pathol 88:95-118, 1977.

47. George JW, Duncan JR: The hematology of lead poisoning in man and animals. Vet Clin Pathol 8:23, 1979.

48. George JW, Duncan JR: Erthrocyte protoporphyrin in experimental chronic lead poisoning in calves. Am J Vet Res 42:1630-1637, 1981.

49. Gerber GB, Leonard A, Jacquet P: Toxicity, mutagenicity and teratogenicity of lead. Mutation Research 76:115-141, 1980.

50. Gerdes AM, Kasten FH: Morphometric study of endomyocardium and epimyocardium of the left ventricle in adult dogs. Am J Anat 159:389-394, 1980.

51. Gilfillan SC: Lead poisoning and the fall of the Roman Empire. J Occup Med 7:53-60, 1965.

52. Goyer RA: Lead toxicity: A problem in environmental pathology. Am J Pathol 64:167-180, 1971.

53. Goyer RA: Intracellular sites of toxic metals. Neurotoxicology 4:147-156, 1983.

54. Goyer RA, Krall R: Ultrastructural transformation in mitochondria isolated from kidney of normal and lead-intoxicated rats. J Cell Biol 41:393-400, 1969.

55. Goyer RA, Mahaffey KR: Susceptibility of lead toxicity. Environ Health perspect 2:73-80, 1972.

56. Goyer RA, Rhyne BC: Pathological effects of lead. Int Rev Exp Path 12:2-77, 1973.

57. Goyer RA, Wilson MH: Lead-induced inclusion bodies: Results of EDTA treatment. Lab Invest 32:149-156, 1975.

58. Granick JL, Sassa S, Granick S, Levere RD, Kappas A: Studies in lead poisoning II. Correlation between the ratio of activated to inactivated delta-aminolevulinic acid dehydratase of whole blood and the blood lead level. Biochem Med 8:149-159, 1973.

59. Graziano JH, Leong JK, Friedheim E: 2,3-dimercaptosuccinic acid: a new agent for the treatment of lead poisoning. J Pharmacol Exp Ther 206:696-700, 1978.

60. Ham AW: Histology. Philadelphia, J B Lippincott Co, 1974, pp 544-548.

61. Hejtmancik M, Williams BJ: Physiological aspects of heavy metal toxicity, in Somani SM (ed): Environmental Toxicology, Principals and Policies. Springfield, IL, Thomas, 1981, pp 45-70.

62. Hejtmancik MR, Williams BJ: Effects of chronic lead exposure on the direct and indirect components of the cardiac response to norepinephrine. Toxicol Appl Pharmacol 51:239-245, 1979.

63. Herbener GH, Swigart RH, Lang CA: Morphometric comparison of the mitochondrial populations of normal and hypertrophic hearts. Lab Invest 28:96-103, 1973.

64. Herdson PB, Sommers HM, Jennings RB: A comparative study of the fine structure of normal and ischemic dog myocardium with special reference to early changes following temporary occlusion of a cornary artery. Am J Pathol 46:367-386, 1965.

65. Hilliard JE: Assessment of sampling error in stereological analysis, in Underwood EE, deWit R, Moore GA (ed): Proceedings Fourth International Congress for Stereology. Washington, National Bureau of Standards, Special Publication 431, US Government Printing Office, 1976, p 59.

66. Jennings RB: Cell volume regulation in acute myocardial ischemic injury. Acta Med Scand Suppl 587:83-92, 1975.

67. Jonek J, Kosmider S, Grzybek H: Histochemical studies on alkaline phosphatase, acid phosphatase, adenosinetriphosphatase and diaphorase in striated muscles and heart muscle in experimental acute lead poisoning. Archivum Immunologiae et Therapiae experimentalis 11:652-663, 1963.

68. Karacic V, Prpic-Majic D, Telisman S: The relationship between zinc protoporphyrin (ZPP) and free erythrocyte protoporphyrin (FEP) in lead-exposed individuals. Int Arch Occup Environ Health 47:165-177, 1980.

69. Karstad L: Angiopathy and cardiopathy in wild waterfowl from ingestion of lead shot. Connecticut Medicine 35:355-360, 1971.

70. Katz AM: Physiology of the heart. New York, Raven Press, 1977.

71. Kehoe RA: The Harben lectures, 1960. The metabolism of lead in man in health and disease. J Roy Inst Publ Health Hyg 24:81-96, 1961.

72. Kehoe RA: Pharmacology and toxicology of heavy metals: lead. Pharmac Ther A 1:161-188, 1976.

73. Khan MY, Buse M, Louria DB: Lead cardiomyopathy in mice. Arch Pathol Lab Med 101:89-94, 1977.

74. Kline TS: Myocardial changes in lead poisoning. Am J Dis Child 99:48-54, 1960.

75. Kloner RA, Ganote CE, Whalen DA, Jennings RB: Effect of a transient period of ischemia on myocardial cells. II. Fine structure during the first few minutes of reflow. Am J Pathol 74:399-422, 1974.

76. Kopp SJ, Perry Jr. HM, Glonek T, Erlanger M, Perry EF, Barany M, D'Agrosa LS: Cardiac physiologic-metabolic changes after chronic low-level heavy metal feeding. Am J Physiol 239 (Heart Circ Physiol 8):H22-H30, 1980.

77. Kosmider S, Petelenz T: Zmiany elektrokardiograficzne u slarszych osob z przewtekym u krolikow. Pol Arch Med weronet 32:437, 1962.

78. Kosmider S, Srocznski J: Zmiany elektrokardiograficzne w przewleklej doswiadczalnej olwixy u krolikow. Postepy Hig Med Dosw 15:353, 1961.

79. Kostial K, Simonovic I, Pisonic M: Lead absorption from the intestine in newborn rats. Nature (Lond) 233:564, 1971.

80. Kowalczyk DF: The value of zinc protoporphyrin in equine lead poisoning: a case report. Vet Hum Toxicol 23:12-15, 1981.

81. Lampert PW, Schochet SS: Demyelination and remylination in lead neuropathy. J Neuropathol Exp Neurol 27:527-546, 1968.

82. Langer GA, Brady AJ (ed): The mammalian myocardium. New York, Wiley and Sons, 1974.

83. Lee WR: What happens in lead poisoning. J Royal College of Physicians of London 15:48-54, 1981.

84. Levander OA: Lead toxicity and nutritional deficiencies. Environ Health Perspect 29:115-125, 1979.

85. Loew FM, Bettany JM, Halifax CE: Apparent thiamin status of cattle and its relationship to polioencephalomalacia. Can J Comp Med 39:291-295, 1975.

86. Louis-Ferdinand RT, Glass L, Sharp R, Beuthin FC: Altered lead distribution in thiamin-treated rodents. Toxicologist 2:82, 1982 (Abstract).

87. Martinez-Palomo A, Alanis J, Benitez D: Transitional cardiac cells of the conductive system of the dog heart. J Cell Biol 47:1-17, 1970.

88. McCallister LP, Daiello DC, Tyers GFO: Morphometric observations on the effects of normothermic ischemic arrest on dog myocardial ultrastructure. J Mol Cell Cardiol 10:67-80, 1978.

89. Merz WA, Schenk RK: Quantitative structural analysis of human cancellous bone. Acta anat 75:54-66, 1970.

90. Mollenhauer HH, Bratton GR, Zmudzki J, Droleskey RE, Rowe LD: An ultrastructural study comparing two potential treatments for lead poisoning in calves. TSEMJ 15:31 1984 (Abstract).

91. Moore MR: Lead and the mitochondrion. Postgrad Med J 51:760-764, 1975.

92. Moore MR, Meredith PA, Goldberg A, Carr KE, Toner PG, Lawrie TDV: Cardiac effects of lead in drinking water of rats. Clin Sci Mol Med 49:337-341, 1975.

93. Moran JR, Greene HL: The B vitamins and vitamin C in human nutrition. Am J Dis Child 133:192-199, 1979.

94. Murakami M, Hirosawa K: Electron microscope autoradiography of kidney after administration of ^{210}Pb in mice. Nature 245:153-154, 1973.

95. Myerson RM, Eisenhauer JH: Atrioventricular conduction defects in lead poisoning. Amer J Cardiol 11:409-412, 1963.

96. Ong CN, Lee WR: Distribution of lead-203 in human peripheral blood in vitro. Br J Industrial Medicine 37:78-84, 1980.

97. Page E: Mammalian ventricular myocardial cells, in Weibel ER, (ed): Stereological Methods. Vol 1. Practical Methods for Biological Morphometry. New York, Academic Press, 1979, pp 284-289.

98. Page E, McCallister LP: Quantitative electron microscopic description of heart muscle cells. Am J Cardiol 31:172-181, 1973.

99. Page E, McCallister LP, Power B: Stereological measurements of cardiac ultrastructures implicated in excitation-contraction coupling. Proc Nat Acad Sci USA 68:1465-1466, 1971.

100. Page E, Polimeni PI, Zak R, Earley J, Johnson M: Myofibrillar mass in rat and rabbit heart muscle: correlation of microchemical with stereological measurements in normal and hypertrophic hearts. Circ Res 30:430-439, 1972.

101. Papadimitriou JM, Hopkins BE, Taylor RR: Regression of left ventricular dilation and hypertrophy after removal of volume overload. Morphological and ultrastructural study. Circ Res 35:127-135, 1974.

102. Pape C, Kubler W, v.Smekal P: Morphometrie am reizleilungssystem und arbeitsmyocard des kalbsherzens. Beitr pathol Anat u allg Pathol 140:23-37, 1969.

103. Partin, JS, Benzing G, Partin JC: Quantitative fine structural changes in dog heart following cardiopulmonary bypass. J Mol Cell Cardiol 4:345-355 (1972).

104. Piomelli S, Rosen JF, Chisolm JJ Jr, Graef JW: Management of childhood lead poisoning. J Pediatr 105:523-532, 1984.

105. Plattner H, Tiefenbrunner F, Pfaller W: Cytomorphometric and biochemical differences between the muscle cells in atria and ventricles of the guinea pig heart. Anat Rec 167:11-16, 1970.

106. Rabinowitz MB, Wetherill GW, Kopple JD: Lead metabolism in the normal man: Stable isotope studies. Science 182:725-727, 1973.

107. Rabinowitz MB, Wetherill GW, Kopple JD: Kinetic analysis of lead metabolism in healthy humans. J Clin Invest 58:260-270, 1976.

108. Robinson TF, Winegrad S: A variety of intercellular connections in heart muscle. J Mol Cell Cardiology 13:185-195, 1981.

109. Sasser LB, Hall GG, Bratton GR, Zmudzki J: Absorption and tissue distribution of lead in thiamin-replete and thiamin-deficient rats. J Nutr 114:1816-1825, 1984.

110. Schiaffino S, Severin E, Hanzlikova V: Intermembrane inclusions induced by anoxia in heart and skeletal muscle mitochondria. Virch Arch B Cell Path 31:169-179, 1979.

111. Scott KM, Hwang KM, Jurkowitz M, Brierley GP: Ion transport by heart mitochondria. XXIII. The effects of lead on mitochondrial reactions. Arch Biochem Biophysics 147:557-567, 1971.

112. Silver W, Rodriguez-Torres R: Electrocardiographic studies in children with lead poisoning. Pediatrics 41:1124-1127, 1968.

113. Singh N, Thind IS, Vitale LF, Pawlow M: Lead content of tissues of baby rats born of, and nourished by lead-poisoned mothers. J Lab Clin Med 87:273-280, 1976.

114. Smigla K, Wazna-Bogunska Cz: Toxic damage to internal organs of guinea-pigs fed fodder containing an admixture of lead. Pat Pol 4:485-491, 1977.

115. Sommer JR, Steere RL, Johnson EA, Jewett PH: Ultrastructure of cardiac muscle. Hibernation and Hypothermia, Perspectives and Challenges. Amsterdam, Elsevier Publishing Co, 1972, pp 291-355.

116. Stofen D: Environmental lead and the heart. J Mol Cellular Cardiology 6:285-290, 1974.

117. Stowe HD, Goyer RA, Krigman MM, Wilson M, Cates M: Experimental oral lead toxicity in young dogs. Arch Pathol 95:106-116, 1973.

118. Tokarski E, Reio L: Effect of lead poisoning on the thiamine status and function in liver and blood of rats. Acta Chemica Scandinavica B 32:375-379, 1978.

119. Underwood EE: Quantitative Stereology. Reading Mass, Addison-Wesley, 1970.

120. US Bureau of Mines. Minerals yearbook 1969: Metals, minerals and Fuels. Washington, US Government Printing Office, 1969, p 638.

121. Warnock LG, Prudhomme CR, Wagner C: The determination of thiamin pyrophosphate in blood and other tissues, and its correlation with erythrocyte transketolase activity. J Nutr 108:421-427, 1978.

122. Weibel ER: Stereological principles for morphometry in electron microscopic cytology, in Bourne GH, Danielli JF (ed): Int Rev of Cytology. Vol. 26. New York, Academic Press, 1969, pp 235-302.

123. Weibel ER: Stereological Methods, Vol 1, Practical Methods for Biological Morphometry. New York, Academic Press, 1979.

124. Weibel ER, Bolender RP: Stereological techniques for electron microscopic morphometry, in Hayat MA (ed): Principles and Techniques of Electron Microscopy. Vol. 3. New York, Van Nostrand Reinhold Co, 1973, pp 237-296.

125. Weibel ER, Kistler GS, Scherle WF: Practical stereological methods for morphometric cytology. J Cell Biol 30:23-38, 1966.

126. Whalen DA, Hamilton DG, Ganote CE, Jennings RB: Effect of a transient period of ischemia on myocardial cells. Am J Pathol 74:381-397, 1974.

127. White DJ, McLeod S: Experimental canine distemper infection as a means of demonstrating latent effects of subacute lead intoxication. Br J exp Path 57:645-652, 1976.

128. Williams BJ, Hejtmancik MR Jr, Abreu M: Cardiac effects of lead. Federation Proc 42:2989-2993, 1983.

129. Williams MA: Quantitative methods in biology in Glauert AM (ed): Practical Methods in Electron Microscopy. Vol 6. Amsterdam, North-Holland Publishing Co, 1977, pp 5-84.

130. Woolley DE: Personal communication. June, 1985.

131. Woolley-Efigenio ND, Woolley DE, Ferrell MF, Dreyfus PM: Effects of thiamin on the neurotoxicity of lead. Abstracts: Society for Neuroscience 9:671, 1983.

132. Yeager DW, Cholak J, Henderson EW: Determination of lead in biological and related material by atomic absorption spectrophotometry. Environ Sci Technol 5:1020-1022, 1971.

133. Zmudzki, J: Oznaczanie zawartosci olowiu w materiale biologicznym metoda spektrofotometrii atomowo-absorpcyjnej. Medycyna Wet 33:179-181, 1977.

134. Zmudzki J, Bratton GR: Blood Pb, ALAD, and ZPP in calves receiving low doses of lead. Toxicologist 4:117, 1984.

135. Zmudzki J, Bratton GR, Womac C, Rowe LD: The influence of milk diet, grain diet, and method of dosing on lead toxicity in young calves. Toxicol Appl Pharmacol 76:490-497, 1984.

APPENDIXES

APPENDIX A

STEREOLOGY

1. STEREOLOGICAL FORMULAS

The first basic stereological method involves determining volume densities V_V using the general formula (124):

$$V_{Vi} = A_{Ai} = P_i/P_c$$

$V_{Vi,c}$ is the volume density of i (which could be mitochondrial volume) which is in the contained space c (cell volume). $V_{Vi,c}$ is equal to the number of points that overlie the object i (P_i) in a micrograph divided by the number of points that overlie the contained space c (P_c). Commonly the total number of points on a micrograph do not fall on the contained space and therefore P_c should be used instead of P_T (the total test point number).

The second basic stereological method involves estimating the surface density S_V (124). A section or slice through an individual component of a solid is a profile and the surface of structures appears on these sections as a boundary trace of the profiles. The length of all the profile boundaries found per unit area of section, B_A, is proportional to S_V where

$$S_V = 4/\pi \times B_A$$

While the length of the boundary trace can be directly measured by fitting a thread to the trace or using a map measuring wheel, it is most efficiently determined with point counting. B_A is proportional to the number of intersections I_L formed by the boundary trace with a test line system of known length L_T:

$$B_A = \pi/2 \times I_L$$

From these two formulas it follows that S_V is directly related to the number of intersections I_i formed with test lines of length L_T:

$$S_V = 2 \times I_i/L_T = 2 \times I_L$$

The objects may have any shape, but they must not be oriented preferentially (structures must be isotropic). The lines of the test system are anistropic and if the structure is also anistropic, error can be introduced. It is possible to use the test system at two orientations (at right angles) to overcome this. Eisenberg (34,35) uses a square lattice test grid oriented at 19° to the fiber axis to

overcome systematic errors in the number of intersection counts on orientated membrane systems.

The third stereological method is used to estimate linear density J_V. The length per unit volume can be determined for tubules, fibers and filaments by considering them as straight or curved lines in space. Their length density J_V is directly proportional to the number of times they intersect the unit area of a random section plane, Q_A (124). The formula:

$$J_V = 2 \times Q_A$$

can be used to determine the length density J_V by counting the number of intersections Q_A the tubules or filaments make with the section plane.

The determinationn of numerical density N_V is more difficult than estimating volume, surface or linear densities. With these three parameters, shape is not important and discrete particles are not necessary (124). This is in contrast to the determination of numerical density and mean caliper diameter $\bar{D}$ where particle shape and size is necessary for the determinations. The formula:

$$N_V = n/A(\bar{D} + t - 2h)$$

can be used to determine the number of particles per unit volume N_V. The symbol n is the number of counted profiles per area n_A, $\bar{D}$ is the mean caliper diameter (mean distance between two opposite, parallel tangent planes), t is the slice thickness and h is the height of the lost polar caps (39). The estimation of D, t and h can be difficult and are truly applicable only for spherical particles (124). Other methods and formulas can be used (124).

The most difficult stereological problem to solve is determining the size of a particular particle or component or the size distribution of these components (39). In many cases, it is a very important parameter to measure. First the particle shape must be determined and procedures are available (39,122,123,124), however, reasonably satisfactory methods are only available for spherical or nearly spherical objects. If the shape is spherical, a mean diameter and size distribution can be established using the methods described by Weibel (122,123,124), Williams (129) and Elias and Hyde (39). The determination of the size distribution of ellipsoids has been described by De Hoff and Bousquet (32). Their axial ratio should be constant and they should be of the same form (128).

2. TEST POINT NUMBERS

The test point number (P_T) is determined by the precision requirements and the approximate volume of the component of interest (V_{Va}). This volume is estimated on a few micrographs of the appropiate magnification (123, pg 99):

$$P_T = (1-V_{Va})/V_{Va} \times 1/S.E.^2 \ (\overline{V_{Va}})$$

The formula is based on the relative expected standard error (S.E.) and gives the number of points required to estimate a given feature with any particular precision.

Coherent double lattice test systems are used to accommodate different point densities and total point numbers need for different structures. Every g-th line of the system is drawn heavier than the others, resulting in two superimposed test point sets. With P_T intersections of the heavy lines (coarse point lattice), there will be a total of

$$P_{T'} = g^2 \times P_T$$

fine line intersections (fine point lattice) in the test system (124). Determining the volume density of a sparse organille V_{Vs}, is accomplished by counting those fine points P'_s that fall on profiles of s

$$V_{Vs} = P'_s/g^2 \times P_T$$

and V_{Vf} of more frequent organelles is determined using the coarse points

$$V_{Vf} = P_f/P_T$$

The test points differ by a constant factor of g^2 which is important when the data is to be expressed as a percent of only one phase of the total tissue. The volume density of rare organelles in the cytoplasm, V_{Vs}*, could then efficiently be found by

$$V_{Vs}* = P'_s/g^2 \times P_c$$

where P'_s are the fine points falling on profiles of s (one needs only to count these) and P_c as the number of coarse points falling on cytoplasm.

An indirect method described by Page et al. (99) for determining the test point number would be to take the measurements by point counting, rotate the grid 19^o, repeat the measurements and then average the results. Additional measurements could be made until doubling the area counted did not significantly alter either the mean or the dispersion of the data obtained and it was clear that the data conformed to a normal distribution (99).

Surface density S_V of components can be estimated by using intersection counting on the lines of coherent square lattice systems. The test line length is related to the test point number (123, pg 116-118)

$$L_T = P_T \times 2d$$

therefore the surface density is obtained by

$$S_V = 2 \times I_L = 2 \times I/L_T = I\ (P_T \times d)$$

The surface density of a component i within the cytoplasm can be determined by finding the test line length contained within the cytoplasm (this follows directly from the number of test points falling on the cytoplasm P_c) (123):

$$L_c = P_c \times 2d$$

so that

$$S_{Vi,c} = I_i/(P_c \times d)$$

To determine the total length of test lines required to estimate S_V, the acceptabe error and the surface density of the component is required. Hilliard (65) produced an error prediction formula for a line intersection count:

$$S.E.\ (S_V)/S_V = \sqrt{2/I_T}$$

where I_T is the total number of intersections counted. Since

$$I_T = 1/2\ S_V \times L_T$$

the total test line length required to achieve a prescribed relative standard error in S_V is:

$$R.E.S.\ (S_V) = [S.E.\ (S_V)]/\bar{S}_V$$

and can be estimated by:

$$L_T = 4/S_V \times R.S.E.^2\ (S_V)$$

As an alternative, a nomogram can be used which relates the test line length to S_V and the expected relative standard error (123).

Square lattices contain an excessive density of lines when compared with the test point density (124). To overcome this, multipurpose test systems devised by Weibel (124) and others have been proposed.

APPENDIX B

ELECTRON MICROSCOPY PROCEDURES

Plastic Mixture

35 ml Araldite 6005
10 ml Epon 812
60 ml DDSA (Dodecenyl Succinic Anhydride or Hardner)

Heat mixture at 80°C for 15 or 20 minutes and then mix well and store. Heat at 80°C for 5 or 10 minutes before use and add DMP, approximately 1 drop (from a 22 gauge needle) per ml of plastic.

Dehydration and Embedding Procedure

2.5% glutaraldehyde in Tyrode's buffer .....overnight
3 washes in buffer.....20 minutes each
1% O_sO_4 in buffer.....2 hours
3 washes in buffer.....20 minutes each
100% alcohol.....1 hour
100% alcohol.....20 minutes
100% alcohol.....20 minutes
100% propylene oxide.....1 hour
100% propylene oxide.....20 minutes
100% propylene oxide.....20 minutes
1:1 propylene oxide to resin mixture (with DMP).....overnight
Evaporate propylene oxide from tissue (in hood).....2 hours
Embed in fresh resin, let set .....overnight
Vacuum oven at 75°C.....until hard

APPENDIX C

VALUES FOR BLOOD LEAD CONCENTRATIONS, ANIMAL WEIGHTS, DELTA-AMINOLEVULINIC ACID DEHYDRATASE ACTIVITY, ZINC PROTOPORPHYRIN LEVELS, TISSUE LEAD CONCENTRATIONS AND STEREOLOGICAL DATA

TABLE C-I

BLOOD LEAD LEVELS[a]

Group	Animal #	Pretreatment[b]	Posttreatment
Control	2	7	9
	6	6	4
	7	7	6
	12	11	6
	16	4	14
		7.0 (1.1)[c,d]	7.8 (1.7)[d]
Pb	1	6	84
	5	8	63
	9	6	80
	11	4	132
	15	3	74
		5.4 (0.9)[d]	86.6 (11.9)[e]
Pb + B_1	3	4	86
	4	4	69
	8	6	103
	10	6	73
	14	3	77
		4.6 (0.6)[d]	81.6 (6.0)[e]

[a] Expressed as µg/dl whole blood.

[b] Overall pretreatment mean is 5.6 (0.5) µg/dl whole blood.

[c] All means +/- SEM given in ( ).

[d,e] Identical superscript indicates no significant difference ($p > 0.05$) while different superscript indicates significant difference ($p < 0.05$) between groups.

TABLE C-II

ANIMAL WEIGHTS[a]

Group	Animal #	Pretreatment Weight	Posttreatment Weight	Weight Difference
Control				
	2	17	18	+1
	6	30	32	+2
	7	29	30	+1
	12	16	19	+3
	16	10	11	+1
		20.4 (3.9)[b]	22.4 (3.9)	+1.6 (0.4)[c]
Pb				
	1	13	10	-3
	5	30	23	-7
	9	23	19	-4
	11	27	26	-1
	15	15	13	-2
		21.6 (3.3)[b]	18.2 (3.0)	-3.4 (1.0)[c]
Pb + B_1				
	3	17	14	-3
	4	24	19	-5
	8	26	18	-8
	10	22	19	-3
	14	16	11	-5
		21.0 (1.9)[b]	16.2 (1.6)	-4.8 (0.9)[c]

[a] Weight expressed in kg.

[b] Means +/- SEM given in ( ).

[c] The difference is significant ($p < .05$).

TABLE C-III

ALAD ORIGINAL DATA[a]

	#	0WK[c]	1WK	2WK	3WK	4WK
Control	2	282	0[b]	346	0	305
	6	501	0	497	0	347
	7	237	0	239	200	193
	12	385	0	299	260	225
	16	366	331	289	274	330
Pb	1	244	4	5	0	6
	5	400	36	7	0	2
	9	208	34	8	9	11
	11	512	78	41	12	8
	15	412	57	17	23	18
Pb + B_1	3	439	70	8	6	6
	4	718	130	7	12	10
	8	226	45	6	9	14
	10	275	96	56	34	17
	14	425	67	3	14	13

	#	5WK	6WK	7WK	8WK	9WK
Control	2	0	308	376	319	414
	6	0	350	460	352	396
	7	166	178	160	0	0
	12	237	0	0	0	0
	16	315	254	213	144	0
Pb	1	0	0	0	0	0
	5	0	0	0	0	0
	9	9	0	0	0	0
	11	3	0	0	0	0
	15	7	7	11	7	0
Pb + B_1	3	14	0	0	0	0
	4	7	10	0	0	0
	8	10	0	0	0	0
	10	23	14	16	32	25
	14	12	22	15	7	0

[a] Expressed as nM PGB/ml RBC/hr.

[b] 0 Means data was not collected.

[c] Data collected at one week intervals.

TABLE C-IV

ZPP ORIGINAL DATA[a]

	#	0WK[c]	1WK	2WK	3WK	4WK
Control	2	0.80	0.00[b]	0.60	0.00	0.60
	6	1.40	0.00	1.10	0.00	0.90
	7	0.80	0.00	0.80	0.80	1.10
	12	1.60	0.00	1.40	1.40	1.30
	16	0.80	0.80	0.50	0.90	0.90
Pb	1	1.60	1.30	1.90	2.10	0.00
	5	1.10	1.20	1.50	1.30	1.40
	9	0.60	1.20	1.20	1.20	1.60
	11	0.90	1.00	0.80	0.80	1.10
	15	0.90	0.90	0.60	0.90	1.10
Pb + B_1	3	0.40	0.60	1.30	1.10	1.40
	4	1.50	1.10	1.90	1.40	1.70
	8	0.70	1.20	1.50	1.40	1.90
	10	0.90	7.90	8.90	7.70	8.00
	14	1.60	1.70	1.40	1.60	1.90

	#	5WK	6WK	7WK	8WK	9WK
Control	2	0.00	0.50	0.80	0.80	0.80
	6	0.00	0.90	1.20	1.80	1.50
	7	0.90	0.90	1.40	1.60	0.00
	12	1.30	0.00	0.00	0.00	0.00
	16	0.70	0.80	0.50	0.60	0.00
Pb	1	0.00	0.00	0.00	0.00	0.00
	5	1.70	1.90	1.60	2.20	3.10
	9	1.10	1.50	0.00	0.00	0.00
	11	1.20	1.90	0.00	0.00	0.00
	15	1.40	1.20	1.60	1.40	0.00
Pb + B_1	3	2.00	2.30	0.00	0.00	0.00
	4	1.90	2.10	2.10	2.50	3.20
	8	2.50	0.00	0.00	0.00	0.00
	10	7.70	7.00	6.90	7.10	0.00
	14	2.40	2.80	2.10	2.90	0.00

[a] Expressed as µg ZPP/Gm Hb.

[b] 0.00 Means data was not collected.

[c] Data collected at one week intervals.

TABLE C-V

TISSUE LEAD CONCENTRATIONS[a]

	#	HRT[b]	M.V	M.B	LIV	KID
Control	2	0.04	0.03	0.01	0.54	0.29
	6	0.05	0.04	0.03	0.25	0.15
	7	0.05	0.04	0.03	0.37	0.28
	12	0.07	0.06	0.05	0.55	0.30
	16	0.10	0.06	0.07	1.88	1.03
Pb	1	0.14	0.24	0.30	46.97	41.97
	5	0.20	0.31	0.21	33.17	12.80
	9	0.32	0.21	0.19	63.16	20.69
	11	0.55	0.31	0.18	61.91	33.91
	15	0.28	0.29	0.31	34.80	18.24
Pb + B_1	3	0.41	0.25	0.43	11.86	13.04
	4	0.40	0.46	0.44	71.09	27.26
	8	0.23	0.16	0.47	56.42	51.08
	10	0.20	0.08	0.16	50.24	11.24
	14	0.63	0.48	0.13	57.45	44.67

	#	B.F	MAR	BIL	BST	COR
Control	2	15.27	1.20	0.19	0.14	0.13
	6	7.88	0.29	0.11	0.12	0.05
	7	5.82	1.60	0.05	0.07	0.13
	12	6.41	0.35	0.07	0.08	0.10
	16	22.38	1.68	0.19	0.11	0.06
Pb	1	78.10	0.00	9.76	0.91	0.83
	5	96.85	3.54	10.17	0.98	3.60
	9	55.03	3.44	10.95	1.44	1.46
	11	77.50	2.68	7.21	0.97	0.93
	15	65.48	4.18	3.01	1.18	1.39
Pb + B_1	3	84.71	0.00	2.15	0.64	1.29
	4	97.78	7.16	4.71	1.39	1.35
	8	95.65	6.94	9.21	0.76	1.00
	10	116.67	4.53	1.83	0.95	1.44
	14	78.79	14.39	16.48	1.06	1.48

[a] Expressed as mg/kg wet weight.

[b] Abbreviations used: HRT-heart, M.V-vastus lateralis muscle, M.B.-biceps muscle, LIV-lever, KID-kidney, B.F.-bone(femoral head), MAR-bone marrow, BIL-bile, BST-brain stem, COR-cerebral cortex.

TABLE C-VI

ADDITIONAL TISSUE LEAD CONCENTRATIONS[a]

	#	CER[b]	NER	SPC	SPL	PAN
Control	2	0.20	0.10	0.11	0.19	0.27
	6	0.12	0.03	0.06	0.05	0.15
	7	0.31	0.05	0.07	0.12	0.07
	12	0.05	0.07	0.12	0.13	0.12
	16	0.16	0.67	0.15	0.29	0.60
Pb	1	0.67	0.68	0.76	7.56	2.38
	5	0.93	0.60	0.66	10.89	2.24
	9	1.11	1.02	0.84	7.90	1.71
	11	0.87	1.11	0.65	4.79	1.75
	15	1.09	0.99	0.87	6.02	2.41
Pb + B_1	3	0.71	0.63	0.17	2.60	1.33
	4	1.12	1.20	1.06	6.26	2.04
	8	0.71	1.26	0.48	8.82	2.46
	10	0.60	0.43	0.49	7.64	1.43
	14	0.59	1.18	0.62	11.73	2.16

	#	TES	LUN
Control	2	0.06	0.07
	6	0.06	0.06
	7	0.05	0.10
	12	0.08	0.09
	16	0.15	0.23
Pb	1	0.69	1.10
	5	0.46	1.16
	9	0.76	1.38
	11	0.75	1.23
	15	0.75	1.33
Pb + B_1	3	0.41	1.12
	4	0.55	1.47
	8	0.58	0.96
	10	0.28	1.19
	14	0.91	1.00

[a] Expressed as mg/kg wet weight.

[b] Abbreviations used: CER-cerebellum, NER-nerve, SPC-spinal cord, SPL-spleen, PAN-pancreas, TES-testes, LUN-lung.

TABLE C-VII

CONTROL STEREOLOGICAL DATA[a]

	MYO[b]	MIT	INT	NUC	LIP	MYE
1	49.57	23.30	27.13	0.00	0.0760	0.2610
2	59.93	18.60	19.86	1.61	0.6710	0.2240
3	57.10	21.68	19.97	1.25	0.2630	0.0290
4	49.33	22.50	26.33	1.83	0.0830	0.0000
5	57.17	23.14	19.52	0.17	0.1840	0.0000
6	56.62	20.70	19.87	1.99	0.1450	0.0210
7	51.66	22.32	23.43	2.58	0.1500	0.0350
8	52.82	23.74	22.37	1.07	0.1050	0.1050
9	56.79	23.21	18.39	1.61	0.1000	0.0000
10	53.14	17.66	27.23	1.98	0.1240	0.0000
11	57.72	22.24	20.03	0.00	0.0420	0.0000
12	53.05	23.05	21.53	2.37	0.0320	0.0000
13	50.56	25.84	19.85	3.75	0.0230	0.0000
14	56.97	21.98	20.59	0.77	0.2900	0.0190
15	57.17	22.43	18.72	1.69	0.0840	0.0000
16	56.63	24.44	15.15	3.79	0.0110	0.0000
17	59.90	22.72	17.38	0.00	0.2040	0.0000
18	51.89	23.96	23.78	0.36	0.0110	0.0450
19	56.43	19.64	23.93	0.00	0.0670	0.0450
20	55.08	26.69	17.86	0.38	0.4350	0.0000
21	55.14	19.94	22.19	2.73	0.3320	0.0400
22	62.27	23.79	13.94	0.00	0.1390	0.0580
23	52.14	24.87	22.98	0.00	0.1180	0.0430
24	50.56	24.17	25.28	0.00	0.0890	0.1490
25	50.57	29.28	17.30	2.83	1.0930	0.0120
26	54.23	22.13	22.56	1.08	0.2440	0.0950
27	58.46	23.38	15.87	2.30	0.0650	0.0000
28	50.30	23.65	24.25	1.80	0.0250	0.0000
29	49.83	22.55	25.70	1.92	0.0110	0.0000
30	54.30	23.16	22.54	0.00	0.0510	0.0000
31	56.36	27.93	14.71	1.00	0.0620	0.1400
32	62.28	21.36	15.57	0.80	0.2000	0.0120
33	65.60	27.79	6.61	0.00	0.1000	0.0140
34	61.08	26.40	11.95	0.58	0.2170	0.0120
35	50.29	28.38	20.38	0.95	0.1430	0.3210
36	53.26	23.37	22.58	0.79	0.0600	0.0000
37	62.44	25.33	11.56	0.67	0.0690	0.0000
38	57.79	19.89	19.89	2.44	0.1170	0.0350
39	51.44	25.99	21.85	0.75	0.0820	0.0590
40	58.61	20.97	18.54	1.87	0.0940	0.0000

TABLE C-VII (CONTINUED)

	MYO	MIT	INT	NUC	LIP	MYE
41	55.51	22.04	21.04	1.40	0.2510	0.0000
42	57.45	24.11	16.08	2.36	0.3100	0.0300
43	54.89	26.49	15.99	2.63	0.0750	0.0890
44	56.26	26.64	16.50	0.60	0.2110	0.0000
45	63.58	24.28	11.48	0.66	0.0690	0.0140

[a] Expressed as percent of cell volume.

[b] Abbreviations used: MYO-myofilaments, MIT-mitochondria, INT-intercellular space, NUC-nucleus, LIP-lipofuscin, MYE-myelin figures.

TABLE C-VIII

PB STEREOLOGICAL DATA[a]

	MYO[b]	MIT	INT	NUC	LIP	MYE
46	60.50	15.05	22.26	2.19	0.0290	0.0000
47	55.16	22.81	21.25	0.78	0.0880	0.0000
48	59.32	22.56	16.75	1.37	0.0640	0.0000
49	60.95	18.15	17.55	3.35	0.1600	0.0250
50	52.72	20.07	26.02	1.19	0.2130	0.0000
51	47.13	21.26	30.31	1.29	0.5660	0.0000
52	57.66	21.35	19.89	1.09	0.1370	0.0000
53	52.33	22.76	24.90	0.00	0.1460	0.0000
54	51.34	24.71	23.75	0.19	0.0720	0.0600
55	53.06	22.26	22.63	2.04	0.2090	0.0000
56	56.46	20.07	20.24	3.23	0.2760	0.0210
57	56.20	21.82	20.42	1.57	0.3930	0.0000
58	60.28	23.86	15.70	0.16	0.0590	0.0390
59	54.91	22.80	22.30	0.00	0.2600	0.0210
60	63.88	24.29	9.39	2.45	0.2040	0.0380
61	59.21	20.58	18.59	1.62	0.2260	0.0000
62	61.12	22.24	15.94	0.70	0.2410	0.0000
63	57.43	24.46	17.93	0.18	0.0680	0.0910
64	65.17	20.94	13.46	0.43	0.0930	0.1470
65	62.09	20.75	16.81	0.34	0.2040	0.0210
66	60.23	18.00	19.97	1.80	0.1230	0.0100
67	54.35	22.74	17.05	5.86	0.0110	0.0000
68	58.81	23.06	15.65	2.47	0.1030	0.0310
69	61.25	22.50	16.25	0.00	0.1000	0.1000
70	58.66	20.67	20.14	0.53	0.1210	0.0000
71	52.03	16.75	29.98	1.23	0.0550	0.0000
72	63.87	18.06	15.64	2.42	0.0120	0.0000
73	65.23	20.53	13.25	0.99	0.0410	0.2480
74	61.90	17.71	19.05	1.33	0.1070	0.0000
75	63.57	21.27	14.25	0.90	0.0140	0.0000
76	54.73	16.14	29.31	0.56	0.1740	0.0460
77	54.95	24.77	19.82	0.45	0.0210	0.0000
78	56.50	21.12	21.66	0.72	0.3610	0.0110
79	56.69	17.72	23.62	1.97	0.3200	0.0000
80	54.62	17.88	25.77	1.73	0.0000	0.0000
81	60.32	26.15	12.61	0.92	0.0720	0.0290
82	57.49	21.59	20.48	0.44	0.2750	0.0140
83	60.00	20.57	17.36	2.08	0.1420	0.1060
84	55.43	24.64	19.02	0.91	0.4300	0.0230
85	58.03	23.09	17.67	1.20	0.2010	0.0250

TABLE C-VIII (CONTINUED)

	MYO	MIT	INT	NUC	LIP	MYE
86	60.69	20.04	18.88	0.39	0.1570	0.0000
87	59.17	21.30	18.93	0.79	0.1480	0.0000
88	66.28	22.40	11.32	0.00	0.1590	0.0290
89	67.09	19.41	12.45	1.05	0.2110	0.0000
90	62.00	22.31	15.50	0.19	0.3900	0.0240
91	65.43	20.65	12.17	1.74	0.1770	0.0410
92	61.78	28.13	9.62	0.48	0.0450	0.0150
93	62.53	23.70	11.96	1.81	0.0560	0.0280
94	60.33	21.59	16.61	1.48	0.1040	0.0230
95	59.72	23.41	15.87	0.99	0.0500	0.0370

[a] Expressed as percent of cell volume.

[b] Abbreviations used: MYO-myofilaments, MIT-mitochondria, INT-intercellular space, LIP-lipofuscin, NUC-nucleus, MYE-myelin figures.

TABLE C-IX

PB + B_1 STEREOLOGICAL DATA[a]

	MYO[b]	MIT	INT	NUC	LIP	MYE
96	49.85	21.05	28.17	0.93	0.0100	0.0000
97	42.95	18.85	36.84	1.36	0.0110	0.0000
98	49.41	25.63	24.11	0.84	0.1050	0.0000
99	47.63	22.63	26.42	3.32	0.1680	0.0000
100	57.81	17.87	23.67	0.64	0.0700	0.0000
101	52.16	25.18	22.66	0.00	0.1800	0.0000
102	57.52	22.56	19.92	0.00	0.0640	0.0000
103	56.40	25.43	17.13	1.04	0.2490	0.0000
104	51.00	25.23	23.77	0.00	0.1470	0.0000
105	59.00	22.99	17.62	0.38	0.1320	0.0240
106	58.92	17.50	22.58	0.98	0.0510	0.0000
107	58.88	21.38	18.91	0.82	0.1440	0.0000
108	59.96	18.60	20.87	0.57	0.0590	0.0000
109	54.19	25.77	19.60	0.44	0.0420	0.0000
110	57.17	22.17	17.82	2.83	0.1250	0.0000
111	53.85	21.96	24.20	0.00	0.0800	0.0000
112	49.73	24.25	26.02	0.00	0.0220	0.0440
113	46.76	25.00	27.88	0.36	0.1570	0.2020
114	52.81	23.97	21.91	1.31	0.0940	0.0350
115	47.25	26.86	22.98	2.91	0.0910	0.0000
116	48.35	19.24	29.11	3.29	0.4110	0.0000
117	55.12	22.01	21.50	1.37	0.1810	0.1070
118	51.62	22.67	22.86	2.86	0.3330	0.0000
119	55.36	21.65	20.11	2.87	0.0720	0.0000
120	54.58	24.06	19.03	2.33	0.1010	0.0000
121	53.08	20.04	25.33	1.54	0.0960	0.0000
122	55.42	18.16	24.76	1.65	0.0880	0.0290
123	54.51	21.72	22.13	1.64	0.0260	0.0130
124	49.63	17.79	32.58	0.00	0.0350	0.0000
125	45.24	19.05	34.39	1.32	0.0330	0.0000
126	58.41	24.28	16.11	1.20	0.1500	0.0300
127	63.32	20.32	14.51	1.85	0.0990	0.0000
128	60.60	26.77	12.63	0.00	0.1340	0.0000
129	53.85	24.73	20.60	0.82	0.4980	0.0000
130	58.87	20.57	18.20	2.36	0.0890	0.0300
131	53.43	17.57	28.12	0.88	0.0660	0.0000
132	60.08	19.56	20.36	0.00	0.1260	0.0000
133	62.65	19.41	16.71	1.23	0.0460	0.0000
134	65.50	16.81	15.28	2.40	0.1090	0.0000
135	64.74	18.38	16.45	0.43	0.0530	0.0000

TABLE C-IX (CONTINUED)

	MYO	MIT	INT	NUC	LIP	MYE
136	56.68	25.71	15.79	1.82	0.0510	0.0130
137	57.98	21.57	19.10	1.35	0.0560	0.0560
138	50.94	26.07	21.78	1.20	0.0860	0.0000
139	50.76	25.00	22.35	1.89	0.1070	0.0360
140	55.14	21.80	22.01	1.05	0.0260	0.0260
141	61.96	23.48	13.04	1.52	0.0680	0.0000
142	62.19	20.61	15.23	1.97	0.0670	0.0780
143	53.75	21.47	23.21	1.57	0.1200	0.0110
144	57.36	20.86	19.37	2.42	0.1630	0.0000
145	58.84	24.16	15.44	1.57	0.4470	0.0420

[a] Expressed as percent of cell volume.

[b] Abbreviations used: MYO-myofilaments, MIT-mitochondria, INT-intercellular space, LIP-lipofuscin, NUC-nucleus, MYE-myelin figures.

VITA

Nancy Gail Kincaid was born in Mesa, Arizona on June 2, 1950. She attended elementary school in Burbank, California. She then attended an elementary and high school in Thousand Oaks, California, graduating from Thousand Oaks High School in 1968. The following September she entered Moorpark Junior College and in January 1970 she transferred to Texas A&M University in College Station, Texas. In June, 1973 she received a Bachelor of Science degree in Biomedical Science.

Nancy pursued graduate studies for two quarters at The University of California at Davis, California and in September 1974 accepted a research and teaching assistantship at Purdue University in the Department of Anatomy. In 1976 she was awarded the Master's degree.

In 1977 she entered the Graduate School of The University of Tennessee at Knoxville. After taking a leave of absence, she was readmitted and received the Doctor of Philosophy degree with a major in Animal Science (Physiology) in August of 1985. The author is a member of Phi Kappa Phi and the American Association of Veterinary Anatomists.

She is married to Dr. Steven A. Kincaid of Sunnyvale, California and has a young daughter, Cheryl Ann.